microorganisms

MDPI

Article

Comparative Growth, Intestinal Microbiota, and Liver Metabolic Profiles of Two Common Carp (*Cyprinus carpio*) Varieties Co-Cultured in a Rice–Fish System Under Fed and Non-Fed Conditions

Mingkun Luo [1,2], Yuanchun Jing [2], Ming Qi [3], Jianjun Fu [1], Lanmei Wang [1], Zaijie Dong [1,2,*] and Wenbin Zhu [1,2,*]

[1] Key Laboratory of Freshwater Fisheries and Germplasm Resources Utilization, Ministry of Agriculture and Rural Affairs, Freshwater Fisheries Research Center, Chinese Academy of Fishery Sciences, Wuxi 214081, China; luomingkun@ffrc.cn (M.L.); fujj@ffrc.cn (J.F.); wanglm@ffrc.cn (L.W.)
[2] Wuxi Fisheries College, Nanjing Agricultural University, Wuxi 214081, China; jingyuanchun2633@163.com
[3] Zhejiang Fisheries Technical Extension Center, Hangzhou 310023, China; qidashuai0632@gmail.com
* Correspondence: dongzj@ffrc.cn (Z.D.); zhuwb@ffrc.cn (W.Z.); Tel.: +86-510-85558831 (W.Z.)

Abstract

Background: The rice–fish co-culture system balances ecological and economic benefits, but whether two carp varieties co-cultured under identical conditions differ in growth, intestinal microecology and liver metabolism remains unclear. Methods: FFRC No. 2 red carp (RF) and Oujiang color carp (OJ) were co-cultured in the same paddy fields and individually identified with passive integrated transponder (PIT) tags; three fields received supplementary feed (F), and the other three did not (NF). Growth, intestinal morphology, intestinal microbiota, metagenomic functions, and the liver metabolome were assessed. Results: RF had greater body length than OJ in both the fed and non-fed fields and a higher weight gain rate than OJ in the fed fields, although the effect of variety on weight gain rate was not significant across fields ($p = 0.081$); OJ had a higher condition factor. Fish sampled from the fed field had larger body dimensions, taller intestinal villi and a higher species richness (Chao1) than those from the non-fed fields, although sequencing depth differed systematically between the two field types and the richness comparison carries that caveat. The functional response to feeding differed between the varieties: in the fed fields OJ was enriched in energy metabolism (TCA cycle), whereas RF showed enrichment of the cell cycle and DNA replication; between the two varieties within the non-fed fields only flagellar assembly was enriched, and none of the 164 differentially abundant genes survived correction (minimum adjusted $p = 0.116$). Integrated analysis indicated associations between intestinal taxa and liver metabolites via purine metabolism and arginine biosynthesis. Conclusions: Under identical co-culture conditions, the two varieties differ consistently in growth and intestinal morphology, whereas the differences in intestinal microbiota and liver metabolism are smaller and, at this sample size, remain exploratory. These observations may inform variety-specific feeding approaches in rice–fish systems.

Keywords: rice–fish co-culture; common carp; feeding management; microbiota; metabolomics

Check for updates

Academic Editor: Wujie Xu

Received: 22 October 2026
Revised: 24 November 2026
Accepted: 24 November 2026
Published: 26 November 2026

Copyright: © 2026 by the authors. Licensee MDPI, Basel, Switzerland. This article is an open access article distributed under the terms and conditions of the Creative Commons Attribution (CC BY) license.

1. Introduction

In recent years, the rapid expansion of aquaculture in both scale and volume has placed significant pressure on the ecological environment. Meanwhile, global population growth is intensifying food security challenges and driving agricultural intensification that heavily relies on chemical inputs, leading to soil degradation and increased pest resistance [1]. Therefore, it is urgent to develop sustainable agricultural models that integrate nutrient cycling and resource-use efficiency to ensure stable food production while minimizing ecological impacts [2]. In this context, the rice–fish co-culture system, which combines rice cultivation with fish farming in paddy fields, represents such a sustainable model by diversifying agricultural outputs and improving land-use efficiency [3]. This system reduces both pest incidence and pesticide application through fish foraging and simultaneously improves soil quality via fish excrement, thereby lowering dependence on chemical fertilizers. This integrated "one-field, dual-use, dual-harvest" approach ultimately yields significant economic and environmental benefits [4,5].

Microorganisms play a pivotal role in the rice–fish co-culture system. Studies have shown that long-term rice–fish co-culture significantly increases soil microbial biomass and organic carbon content, enhances microbial functions such as nitrogen fixation and pollutant degradation, and improves soil fertility [6,7]. Moreover, in this system, bacterial community diversity in sediments is higher, while heavy metal content and release, as well as pathogen abundance, are reduced [8]. The intestinal microbiota of fish is also influenced by this system. Compared with traditional pond aquaculture, the intestinal microbiota of carp reared in rice paddies has been reported to contain a lower relative abundance of sequences assigned to taxa that include known pathogens, together with a more diverse and more stable intestinal microbial community [9,10].

Common carp (*Cyprinus carpio*), a major freshwater aquaculture species worldwide, is characterized by strong disease resistance, rapid growth and high adaptability. As an omnivorous fish, it can filter-feed on natural food sources, making it an ideal species for rice–fish co-culture systems, where it helps control weeds and pests in paddy fields. In traditional rice–fish co-culture, artificial feed supplementation is minimal. However, studies have indicated that supplementary feeding can increase yields of both fish and rice. Unconsumed feed acts as an organic fertilizer, with its nitrogen gradually becoming available for uptake by rice plants [11]. Although this benefit has been observed, the underlying mechanisms-particularly those mediated by microorganisms-remain poorly understood. In addition, the impact of feed input on paddy microecology requires further evaluation. As demonstrated by Diao et al. [12], feed used in rice–fish co-culture increases water nutrient levels, which in turn reduces bacterial diversity, weakens microbial interactions, and leads to a more unstable network structure.

This study selected two common carp varieties. One is the red FFRC No. 2 strain, derived from the FFRC No. 2 common carp line, which has passed national certification and described in its breeding records as fast-growing with a well-proportioned body shape. The other is the Oujiang color common carp, a unique strain that has been cultivated for approximately 1200 years in the rice–fish co-culture system of the Oujiang River basin in Zhejiang Province, China [13]. Few studies have compared carp growth, intestinal microbial diversity and liver metabolic profiles under different feeding regimes in the rice–fish co-culture model. The present study therefore compares the growth performance, the composition and function of the microbial community in the rearing environment and in the fish intestine, and the liver metabolic profile of these two carp varieties under fed and non-fed conditions, and examines the associations between the intestinal microbiota and both the environmental microbial communities and the liver metabolites. Because the feeding regime was applied at the field scale, the variety contrast provides the inferential

basis of the study, whereas the between-field comparisons are reported as descriptive observations. The findings are intended to clarify how the two varieties differ under identical co-culture conditions and to identify questions for future, replicated field experiments; they do not constitute a quantitative assessment of feeding practice, feed efficiency or economic performance.

2. Materials and Methods

2.1. Animal Ethics Statement

All experimental procedures were reviewed and approved by the Animal Care and Use Committee of the Freshwater Fisheries Research Center (FFRC), Chinese Academy of Fishery Sciences (CAFS) (approval No. ACUC-FFRC-2024-04-03, April 2024). The experiment was conducted from April 2024 to December 2025 in accordance with the committee recommendations (BC2013863, 9/2013) and with the relevant guidelines and regulations issued by the Ministry of Science and Technology, Beijing, China (No. 398, 2006).

2.2. Experimental Materials

In this study, the initial average body weight of Oujiang color common carp was 73.70 ± 2.23 g (designated as OJ, sourced from Qingtian Yugong Agriculture Technology Co., Ltd., Lishui, China), and the initial average body weight of the red FFRC No. 2 strain common carp was 68.10 ± 2.17 g (designated as RF, sourced from FFRC, CAFS, Wuxi, China). A rice–fish co-culture experiment was conducted under mountainous conditions in Wuyishan, China, using six paddy fields (666.67 m^2 each) that were separated by bunds and managed identically except for the feeding treatment: three fields were assigned to feeding management (labeled F1, F2 and F3), and the other three received no supplementary feeding throughout the experiment (labeled NF1, NF2 and NF3). Because the fields were physically separate, fish could not move between them, and neither variety was distributed naturally. Each paddy field was stocked with 100 individuals of each variety (200 fish per field), and all individuals were identified by abdominal injection of passive integrated transponder (PIT) tags. During the experiment, the water temperature ranged from 25 to 28 °C, the pH from 7.0 to 8.0, and the dissolved oxygen concentration from 4 to 6 mg/L. The feed used in the feeding fields was a commercial extruded pellet for carp (particle size 3 mm, crude protein content 28%) that contains fish meal. Feeding was carried out once daily in the evening, with no feeding on rainy or overcast days. Survival was calculated for each variety in each field as the number of fish recovered at the end of the experiment divided by the 100 individuals stocked.

After 64 days of feeding, 20 OJ carp and 20 RF carp were randomly selected from each paddy field. The fish were anesthetized with a 0.1 g/L solution of tricaine methanesulfonate (MS-222) (Cat. No. E10521, Sigma-Aldrich, St. Louis, MO, USA). The body weight, body length, body height, and body thickness of each individual were measured. Three fish per variety from each field were then randomly selected for intestinal content collection. The intestines were incised longitudinally with sterilized surgical scissors, and all contents were collected into sterile microcentrifuge tubes; the samples were immediately flash-frozen in liquid nitrogen. The intestinal tissues were then preserved in 4% neutral paraformaldehyde for histological examination. Water samples were collected with a sterile water sampler. Approximately 3 L of water were collected from three randomly selected sampling points in each paddy field at a depth of ~10 cm. The water was immediately filtered on-site through a 0.22 μm pore-size sterile mixed cellulose ester membrane (Merck Millipore Ltd., Carrigtwohill, Ireland) using a portable vacuum pump. The filtration apparatus was sterilized with 75% ethanol between samples. The membranes containing the captured

microbial biomass were aseptically placed into sterile 2 mL cryotubes using sterilized forceps and immediately flash-frozen in liquid nitrogen.

Sediment samples were collected at three random points within each paddy field using sterile grab samplers. The top 1–2 cm of the sediment core was carefully collected after removing the surface layer that had been in contact with water. The sediment was placed into sterile 50 mL centrifuge tubes using a sterile spatula. The tubes were filled quickly to minimize air space, sealed, and immediately immersed in liquid nitrogen. All frozen samples were then transferred to the laboratory and stored at −80 °C until analysis.

2.3. Histological Analysis

After fixation in 4% neutral paraformaldehyde for 24 h, mid-intestinal tissues from the fed and unfed groups were dehydrated, embedded in paraffin, and sectioned into 4 μm slices using a pathology slicer (RM2016, Leica Biosystems, Nussloch, Germany). Neutral paraformaldehyde was selected for its compatibility with downstream immunohistochemistry and immunofluorescence; although Bouin's or Carnoy's fixatives better preserve the mucus layer and fine epithelial detail, 4% neutral paraformaldehyde is sufficient for routine H&E-based morphometry of villus height and width. The sections were stained with hematoxylin and eosin (H&E) and observed under an inverted microscope (IX7, Olympus Corporation, Tokyo, Japan) for imaging. For each fish, three sections were prepared and ten villi were randomly selected from each section (30 villi per fish); the mean of these measurements was used as the value for that fish, and the three fish within each field were averaged to give one field-level replicate.

2.4. 16S rRNA Sequencing

Samples from three randomly selected sampling points in each field were combined into a single sample, and total microbial DNA was extracted from the water and sediment samples using the ALFA-SEQ Water DNA Kit and ALFA-SEQ Soil DNA Kit (Findrop, Guangzhou, China), respectively, following the manufacturer's instructions. DNA quality was assessed using a NanoDrop spectrophotometer (Thermo NanoDrop One, Madison, WI, USA), and DNA concentration was quantified by a fluorometric method (Qubit 3.0 Fluorometer, Thermo Scientific, Waltham, MA, USA). The V3–V4 hypervariable region of the bacterial 16S rRNA gene was amplified using barcoded primers 341F and 805R [14]. PCR was performed in a 50 μL reaction system containing 25 μL of 2× Premix Taq, 1 μL of each primer (10 μmol/L), 3 μL of DNA template, and 20 μL of ddH2O under the following thermal conditions: 94 °C for 5 min; 30 cycles of 94 °C for 30 s, 52 °C for 30 s, and 72 °C for 30 s; and a final extension at 72 °C for 10 min. Amplification products were verified by 1% agarose gel electrophoresis, and target fragments were purified using a gel extraction kit for library construction. The amplicon libraries were sequenced on an Illumina HiSeq 2500 platform (PE250) by Guangdong Magigene Biotechnology Co., Ltd. (Guangzhou, China).

High-quality sequences were clustered into operational taxonomic units (OTUs) at a 97% similarity threshold using UCLUST v1.2.22 [15]. Before clustering, sequences shorter than 110 bp or with an overlap of less than 10 bp were removed, and chimeric sequences were identified and filtered using USEARCH v8.1.1 [16]. Taxonomic assignment of the 16S rRNA gene sequences was performed against the SILVA 16S rRNA database (v138) using UCLUST, with a confidence threshold of 90%. Finally, an OTU table was generated to summarize the abundance profiles of microbial taxa for subsequent analysis. After quality filtering, length filtering, and chimera removal, the water samples retained 94,786–111,203 reads (mean 101,851) corresponding to 4549–5652 non-empty OTUs per sample, and the sediment samples retained 90,829–98,318 reads (mean 95,010) corresponding to 9228–10,086

non-empty OTUs per sample; sequencing depth was therefore comparable across samples within each habitat.

2.5. Metagenomic Sequencing

We first pooled the gut contents from three OJ individuals in each rice paddy into one sample and the gut contents from three RF individuals into another sample. We then extracted microbial genomic DNA from each sample using the ALFA-SEQ Stool High Output DNA Kit (Findrop, Guangzhou, China) according to the manufacturer's protocol. DNA quality was assessed using a NanoDrop spectrophotometer, and DNA concentration was quantified by a fluorometric method. Qualified samples were subjected to shotgun metagenomic sequencing. Dual-indexed sequencing libraries were prepared using the NEBNext® Ultra™ DNA Library Prep Kit for Illumina (NEB, Ipswich, MA, USA) and sequenced on an Illumina HiSeq 2500 platform (PE150) by Magigene Biotechnology Co., Ltd. (Guangzhou, China). Raw reads ranged from 66.0 to 92.9 million per sample (mean 73.5 million), the proportion of bases with a Phred quality score of 30 or more (Q30) ranged from 92.8% to 98.9%, and GC content ranged from 36.0% to 53.0%; per-sample values are given in Table S1. In the revised Supplementary Tables, sample identifiers were standardized to feeding treatment plus field number followed by variety (e.g., F1_OJ denotes variety OJ from the first fed paddy field), so that each identifier specifies its experimental unit. Two degraded primary aliquots from fed field 3 (F3) were replaced before sequencing; the identifiers of the replacement samples have been unified between Tables S1 and S6.

Raw reads were processed with fastp [17] to obtain high-quality clean reads. Filtering comprised removal of adapter sequences, removal of low-quality bases, a 50-bp minimum length and removal of PCR duplicates (fastp parameters: -5 -W 5 -M 20 -q 15 -u 40 -l 50 –dedup). The number of clean reads retained per sample varied widely (0.21 to 66 million) and differed systematically between the fed and non-fed fields, as reported in Table S1. Seven libraries retained fewer than 0.5 million clean reads after filtering (0.28–0.70% of raw reads), whereas five retained 18–66 million; the low-yield libraries also had lower Q30 values (92.8–96.1% versus 97.6–98.9%), indicating that a larger fraction of their raw reads was of low quality. The same trimming parameters were applied to all twelve libraries, so the variation reflects library yield and sequencing output rather than different filtering criteria. De novo assembly of these clean reads was performed using MEGAHIT v1.0.6 [18] to generate Scaftigs (≥500 bp). Open reading frames (ORFs) were predicted from the Scaftigs using Prodigal v2.6.3 [19]. The resulting ORFs were dereplicated and clustered with Linclust v2.0 [20] to construct a non-redundant gene catalog (Unigenes), with the longest sequence from each cluster serving as the representative. Clean reads were then aligned back to this Unigenes catalog using bbmap to calculate gene abundance across samples. These values describe the relative abundance of genes in the metagenome, and therefore the functional potential encoded by the community; they do not measure gene expression or pathway activity, and the functional results are interpreted accordingly. Genes showing differential abundance between groups were identified with DESeq2 using $|\log2(\text{fold change})| > 1$ and a nominal $p < 0.05$; Benjamini–Hochberg adjusted p values were computed for every gene and are reported alongside the nominal values in the Supplementary Tables. Representative gene sequences were aligned to the NCBI NR database using BLAST v2.2.28 (http://blast.ncbi.nlm.nih.gov/Blast.cgi, accessed on 10 May 2025) and taxonomically annotated via DIAMOND v0.9.14 [21] against the RefSeq database. Microbial taxa with relative abundance ≥0.01% in ≥50% of samples were retained. Functional annotation was performed using DIAMOND against the Kyoto Encyclopedia of Genes and Genomes (KEGG) database (v94.2).

2.6. Metabolome Analysis

Similarly, we first pooled the liver samples from OJ and RF fish collected from each field, and then analyzed each pooled liver sample using non-targeted LC-MS metabolomics. For each group, 80 mg of liver tissue was weighed and homogenized with an extraction solvent consisting of methanol and acetonitrile (1:1, v/v). After centrifugation at 4 °C for 15 min at 14,000 g, the supernatant was evaporated under reduced pressure in a vacuum concentrator and then transferred to LC-MS vials for subsequent analysis.

LC-MS analysis was performed on an ultra-high-performance liquid chromatography (UHPLC) system (Agilent Technologies, lnc. Waldbronn, Germany). A 2 µL aliquot of each sample was injected into an amide column (186004801, Waters, Ireland), with the column maintained at 25 °C and a flow rate of 0.5 mL/min. The mobile phase consisted of solvent A (25 mM ammonium acetate and 25 mM ammonium hydroxide in water) and solvent B (acetonitrile). The gradient elution started by decreasing acetonitrile from 95% to 65%, then from 65% to 40%, followed by a 1-min hold at 40% acetonitrile, and then a linear increase back to 95%, with a final hold at 95%. To ensure system stability and data reliability, quality control (QC) samples were included in each run.

Mass spectrometry data were acquired using a mass spectrometer (TripleTOF™ 6600, Sciex, Framingham, MA, USA). A 2 µL sample was injected into a T3 column (186003539, Waters, Ireland) for analysis. The flow rate was set to 0.3 mL/min, and the column temperature was maintained at 25 °C. In positive ion mode, the mobile phase consisted of A = 0.1% formic acid in water and B = 0.1% formic acid in acetonitrile. In negative ion mode, the mobile phase was A = 0.5 mM ammonium fluoride in water and B = acetonitrile. The gradient was set as follows: B was kept at 1% for 1.5 min, then increased linearly to 99% at 11.5 min, held for 3.5 min, and then decreased to 1% at 15 min, with a final 3.4-min hold at 1%. ESI parameters included ion source gas flow rates of 60 psi, curtain gas flow rate of 30 psi, an ion spray voltage (ISVF) of ±5500 V (positive and negative modes), and a gas heater temperature of 600 °C. Information-dependent acquisition (IDA) mode was used for high-sensitivity product ion scanning.

Raw metabolomic data were converted to mzXML with ProteoWizard [22] and processed with XCMS for peak detection, retention-time alignment and correction; missing values were filled and the total peak area of each sample was used for normalization, with features showing a missing rate greater than 50% across samples removed. Metabolite identities were assigned by searching the in-house spectral library of Novogene (Beijing, China), and functional annotation was then performed against the KEGG database. Each annotation carries a confidence level (Level 1, Level 2 or Level 3, where Level 3 denotes an MS1-based annotation for which no MS2 match score was obtained); 1186 metabolites were identified in positive ion mode (202 Level 1, 511 Level 2, 473 Level 3) and 677 in negative ion mode (76 Level 1, 276 Level 2, 325 Level 3). The complete annotation table, including mass error and, where available, the MS2 matching score, is provided in the MetaboLights deposition (MTBLS15304). Quality control. Pooled QC samples were prepared by mixing equal volumes of all experimental samples and were injected before, during and after the analytical run to monitor system stability; all samples were analyzed within a single analytical batch, so no batch correction was applied. Across the three QC injections contained in the quantification table, the median coefficient of variation was 6.3% in positive ion mode and 5.8% in negative ion mode, and 80.0% and 85.2% of the annotated features, respectively, had a coefficient of variation below 15%. No independent validation of individual metabolites (analysis of authentic standards or targeted quantification) was carried out, and the reported metabolite identities should therefore be regarded as library-based annotations rather than confirmed structures. Multivariate analysis, including principal component analysis (PCA), partial least squares discriminant analysis (PLS-DA), and loading plots,

was used to assess sample relationships, remove outliers and identify potential biomarkers; PLS-DA models used one predictive component on autoscaled data, and no orthogonal signal correction was applied. Because only three biological replicates were available per group, model quality was assessed by the goodness of fit (R2Y) and the leave-one-out cross-validated predictive ability (Q^2Y), and overfitting was evaluated by a permutation test in which all $C(6,3) = 20$ distinct two-group label assignments of six samples were enumerated. Metabolites with variable importance in projection (VIP) ≥ 1 and $p < 0.05$ were considered differentially abundant metabolites (DAMs); their Benjamini–Hochberg adjusted p values (q) are reported and a metabolite was regarded as significant after correction only at $q < 0.05$. The reported p values are therefore nominal, and at this sample size the analysis has low power to detect genuine differences. Pathway enrichment analysis of DAMs was conducted using Fisher's exact test, followed by pathway visualization in the KEGG database; enrichment of a pathway indicates the over-representation of annotated metabolites within that pathway and is not, by itself, evidence that the pathway is regulated.

2.7. Joint Analysis of Metagenomics and Metabolomics

Genes with differential abundance in the metagenome and metabolites with differential abundance were mapped to KEGG pathways, and shared pathways were selected for analysis. Correlation analyses were then performed between the abundances of these genes and those of the microbial taxa with differential abundance. Only positive correlations with a nominal $p < 0.05$ were retained, and Benjamini–Hochberg adjusted p values were computed for all correlations tested. Among these pairs we further retained only gene sequences confirmed to be present in the corresponding microbial genomes in the NCBI database. Finally, the relationships among microbial taxa, functional genes and metabolites were visualized with a Sankey diagram.

2.8. Data Analysis

Statistical analysis was performed using SPSS 26.0 (IBM, Armonk, NY, USA). Growth traits were assessed in 120 individually PIT-tagged fish (10 fish per variety per field; 60 per variety in total). Because the feeding regime was applied at the field level, it is completely confounded with field identity; the comparison of the two varieties within the same feeding treatment was pre-planned as the contrast of interest and is treated as inferential, whereas comparisons between fed and non-fed fields are reported descriptively. For intestinal histology, three fish per variety per field were measured (18 fish per feeding treatment; 36 in total; three sections and 30 randomly selected villi per fish); fish means were averaged within each field and the field mean was used as the experimental unit ($n = 3$ fields per feeding treatment). For metagenomic and metabolomic analyses, intestinal contents or liver tissue from three fish of each variety in each field were pooled into one sample, giving three independent samples per group, each corresponding to one paddy field. For the 16S rRNA analysis of water and sediment, three sampling points in each field were pooled into one composite sample ($n = 3$ composite samples per habitat per treatment). For brevity, the four groups compared below are denoted F_OJ and F_RF (fish sampled from the fed fields) and NF_OJ and NF_RF (fish sampled from the non-fed fields). Growth traits (body length, body thickness, body height, weight gain rate and condition factor) and intestinal morphometric indices were analyzed by two-way ANOVA with feeding regime and variety as fixed factors. Individual fish were the unit of observation for growth traits (10 fish per variety per field, nested within field; 30 per variety per feeding treatment), and field means were used for morphometry ($n = 3$ per treatment). Because the feeding regime is identical to field group, the feeding term serves only to absorb field-level variation and its F test is not interpreted; the variety term and the feeding × variety interaction are the terms

of interest, and the variety contrast is made within fields. Because the feeding × variety interaction was not significant for any variable, the variety contrast was resolved within each feeding treatment by Fisher's LSD test (protected LSD), using the pooled error term and residual degrees of freedom of the same two-way model (df = 116 for growth traits, df = 8 for morphometric indices); the two within-treatment variety contrasts per variable were pre-planned, and no further multiplicity adjustment was applied. WGR was calculated as (final body weight − initial body weight)/initial body weight × 100. Data are expressed as mean ± standard error (SE), and Levene's test was used to assess homogeneity of variances. Survival was calculated for each variety in each field (12 field × variety values, three per feeding treatment); the two varieties were compared by pairing them within the same field (paired *t*-test across the six fields), and survival in the fed and non-fed fields is reported descriptively because feeding is confounded with field identity.

The Chao-1 and Shannon indices for water and sediment samples were reported descriptively as means of subsamples. Beta diversity was assessed using permutation-based multivariate analysis of variance (PERMANOVA) based on Bray–Curtis dissimilarity, and homogeneity of dispersion was tested using permutation-based multivariate dispersion analysis (PERMDISP). For gut metagenomic communities, genus- and species-level relative abundance tables were used, and total multivariate variance was decomposed across carp breed, feeding regimen, and their interaction. For water and sediment communities, OTU- and family-level relative abundance tables were used. *p*-values for differentially abundant taxa, genes, and metabolites were corrected for multiple comparisons using the Benjamini–Hochberg false discovery rate (FDR) procedure; for metagenomic gene sets, DESeq2's default independent filtering was applied, and genes excluded by this step were reported with their uncorrected *p*-values but not with corrected *p*-values. For Linear Discriminant Analysis (LDA) effect size (LEfSe) biomarker analysis, no multiple comparison correction was performed; therefore, the results are presented as nominal taxonomic indicators rather than as significance tests.

3. Results

3.1. Effects of Different Feeding Regimens on the Water and Sediment Microbial Communities

Our analysis of water microbial communities revealed no appreciable differences in the Shannon and Chao1 indices between the F and NF fields (Figure 1A,B). PCoA indicated that water communities from different fields were visually distinct (Figure 1C). PERMANOVA based on Bray–Curtis dissimilarity yielded a pseudo-F value of 2.14 and R^2 of 0.349 ($p = 0.30$) at the OTU level, and a pseudo-F value of 1.61 and R^2 of 0.287 ($p = 0.30$) at the genus level (Table S2). In terms of community composition, the dominant phyla in both groups were similar, consisting primarily of Proteobacteria, Actinobacteriota, Bacteroidota, and Patescibacteria (Figure 1D). At the genus level, community compositions were also similar, with dominant taxa including unclassified genera of the Microbacteriaceae and Comamonadaceae families, as well as Polynucleobacter, Sediminibacterium, and Limnohabitans. In contrast, the relative abundances of Limnohabitans, Pseudarcicella, and unclassified genera of Sporichthyaceae were higher in water from NF fields, whereas water from F fields were enriched in an unclassified genus of Microbacteriaceae and Aurantimicrobium (Figure 1E). LEfSe analysis identified indicator taxa that were nominally more abundant in the F water samples, including Aurantimicrobium, actinobacterium MWH, and Sphingobacterium, and 14 taxa that were nominally more abundant in the NF water samples, such as Arcicella sp., Pseudarcicella, Novosphingobium, and Flavobacterium aciduliphilum (Figure 1F; Table S3).

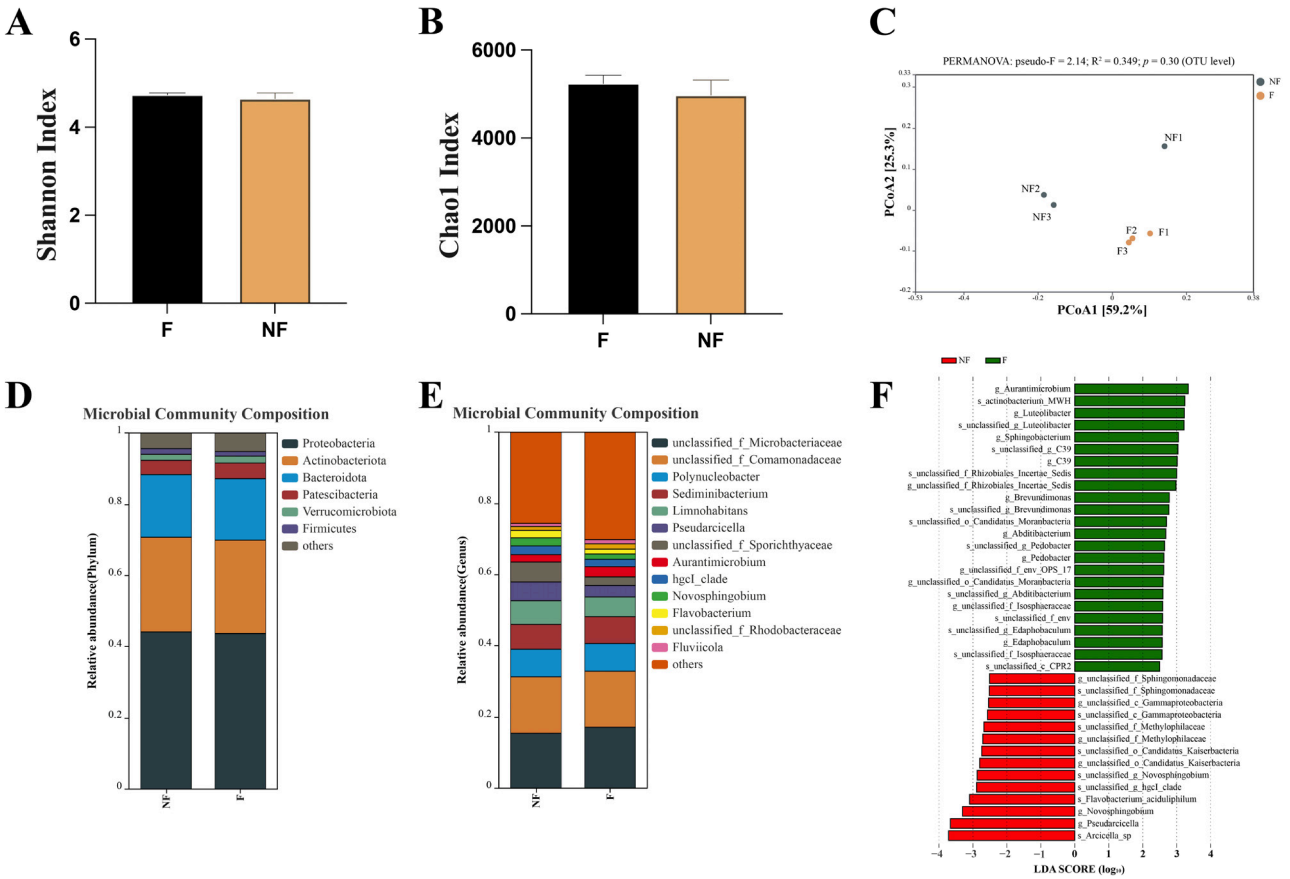


Figure 1. Differences in the diversity and composition of water microbial communities in type F and type NF rice–fish co-culture systems. (**A**) Alpha diversity of water microbiota assessed using the Shannon index; (**B**) Alpha diversity of water microbiota assessed using Chao1 index; (**C**) Beta diversity analyzed by PCoA based on Bray–Curtis distances; PERMANOVA of the same dissimilarities did not reach $p < 0.05$ (water: pseudo-F = 2.14, $R^2 = 0.35$, $p = 0.30$ at OTU level). (**D**) Relative abundance of water microbial communities at the phylum levels; (**E**) Relative abundance of water microbial communities at the genus levels. (**F**) LEfSe analysis identifying nominally differentially abundant taxa between F and NF rice–fish co-culture systems (LDA score > 2.5; $n = 3$; no correction for multiple testing was applied).

There were also no appreciable differences in the Shannon and Chao1 indices of sediment microbial communities between the two feeding treatments (Figure S1A,B). PCoA cluster analysis likewise indicated that sediment communities from different experimental plots tended to be distinct (Figure S1C). PERMANOVA based on Bray–Curtis dissimilarity reached the resolution limit of this experimental design (genus level: pseudo-F = 2.81, $R^2 = 0.412$, $p = 0.10$; OTU level: pseudo-F = 2.13, $R^2 = 0.347$, $p = 0.10$): because this design did not achieve a significance level of $p < 0.05$, these results are reported as trends rather than statistically significant differences. In terms of community composition, the dominant phyla in both sediment groups were similar, consisting primarily of Chloroflexi, Proteobacteria, Acidobacteriota, Bacteroidota, and Verrucomicrobiota (Figure S1D). At the genus level, the community structures were also comparable, being composed predominantly of unclassified genera from the families Pedosphaeraceae and Anaerolineaceae, as well as the class Anaerolineae. Comparative analysis showed that the relative abundances of unclassified genera from the orders RBG-13-54-9 and Acidobacteriales were higher in the NF field sediments than in the F field (Figure S1E). LEfSe analysis identified 13 indicator taxa that were nominally more abundant in the F sediment and 14 in the NF field sediment, such as unclassified species of the RBG order, and unclassified genera and species of the order

Acidobacteriales, among others (Figure S1F; Table S3). Because a three-versus-three comparison admits only 20 distinct label assignments, the minimum attainable permutation p is 0.10 and $p < 0.05$ cannot be reached in this design (Table S2); the indicator taxa listed above and in Figure S1F are therefore nominal results of an uncorrected LEfSe analysis rather than statistically supported differences, and they are reported as exploratory observations only.

3.2. Effects of Different Feeding Regimens on Growth Performance and Intestinal Morphology

Survival was recorded for every fish at the end of the experiment and is reported per field, because the field is the unit to which the feeding treatment was applied. Across the 12 field × variety combinations (Table S4), survival ranged from 71% (NF1, OJ) to 89% (F1, RF) and averaged 81.8% over the six fields (981 of 1200 fish); group means were 81.3% for F_OJ (F1 76%, F2 85%, F3 83%), 84.3% for F_RF (89%, 81%, 83%), 78.7% for NF_OJ (71%, 86%, 79%) and 82.7% for NF_RF (78%, 88%, 82%). Pairing the two varieties within each field, the variety difference was not significant (mean difference 3.5 percentage points; 95% CI −2.7 to 9.7; paired t = 1.46, df = 5, $p = 0.21$), and survival in the fed and non-fed fields was similar (82.8% vs. 80.7%): as with the other between-field contrasts, the latter is descriptive only, since feeding is confounded with field identity. Growth traits were analysed as described in Section 2.8; within each feeding treatment the two varieties were compared by Fisher's LSD test (30 fish per variety per treatment), which is the pre-planned contrast of interest and the only comparison treated as inferential (Figure 2). The interaction between feeding regime and variety was not significant for any of the five traits ($p = 0.20$–0.83). Within the fed fields, RF carp were longer than OJ carp (LSD $p = 0.005$; Figure 2A), had a higher WGR (LSD $p = 0.033$; Figure 2D) and a lower condition factor (LSD $p < 0.0001$; Figure 2E); within the non-fed fields the same direction was observed for body length (LSD $p = 0.002$; Figure 2A) and the condition factor (LSD $p < 0.0001$; Figure 2E), whereas WGR did not differ between varieties (LSD $p = 0.75$; Figure 2D). Body thickness (LSD $p = 0.77$ and 0.41; Figure 2B) and body height (LSD $p = 0.78$ and 0.13; Figure 2C) did not differ between varieties in either treatment. Considered across treatments, the variety main effect was significant for body length ($p = 0.00004$) and the condition factor ($p < 0.0001$) but not for body thickness ($p = 0.70$), body height ($p = 0.39$) or WGR ($p = 0.081$); for WGR, therefore, the difference seen in the fed fields is reported as a treatment-specific observation rather than as a general variety effect. Fish sampled from the fed fields were larger and grew faster than those sampled from the non-fed fields (mean weight gain rate 211% vs. 98%; Figure 2). Because the feeding treatment was applied at the field level, with three fields per treatment, these between-field contrasts are descriptive: no inferential test is claimed for them, and they are not attributed to feeding alone.

H&E-stained tissue sections revealed distinct differences in intestinal structure among the groups ($n = 3$ fields per feeding treatment; Figure 3A). Villus height was greater in fish sampled from the fed fields than in those from the non-fed fields, and within the fed fields it was greater in RF than in OJ (LSD $p = 0.034$; Figure 3B). Regardless of field, villus width was greater in RF than in OJ (fed fields: LSD $p = 0.013$; non-fed fields: LSD $p = 0.033$; Figure 3C). Within each variety, villus width did not differ appreciably between the fed and non-fed fields; this between-field contrast is descriptive and is not bracketed in Figure 3C. Tunica muscularis thickness did not differ appreciably among the groups (Figure 3D). The interaction between feeding regime and variety was not significant for any of the three measurements ($p = 0.26$–0.69). Across both feeding treatments, the variety main effect was significant for villus height ($p = 0.035$) and villus width ($p = 0.004$) but not for tunica muscularis thickness ($p = 0.16$). Mean villus height was 476 µm in fish from the fed fields and 350 µm in those from the non-fed fields, whereas villus width (55 vs. 51 µm) and tunica muscularis thickness (71 vs. 70 µm) were similar. As with the growth traits, the fed-versus-non-fed contrasts are descriptive and are not attributed to feeding alone.

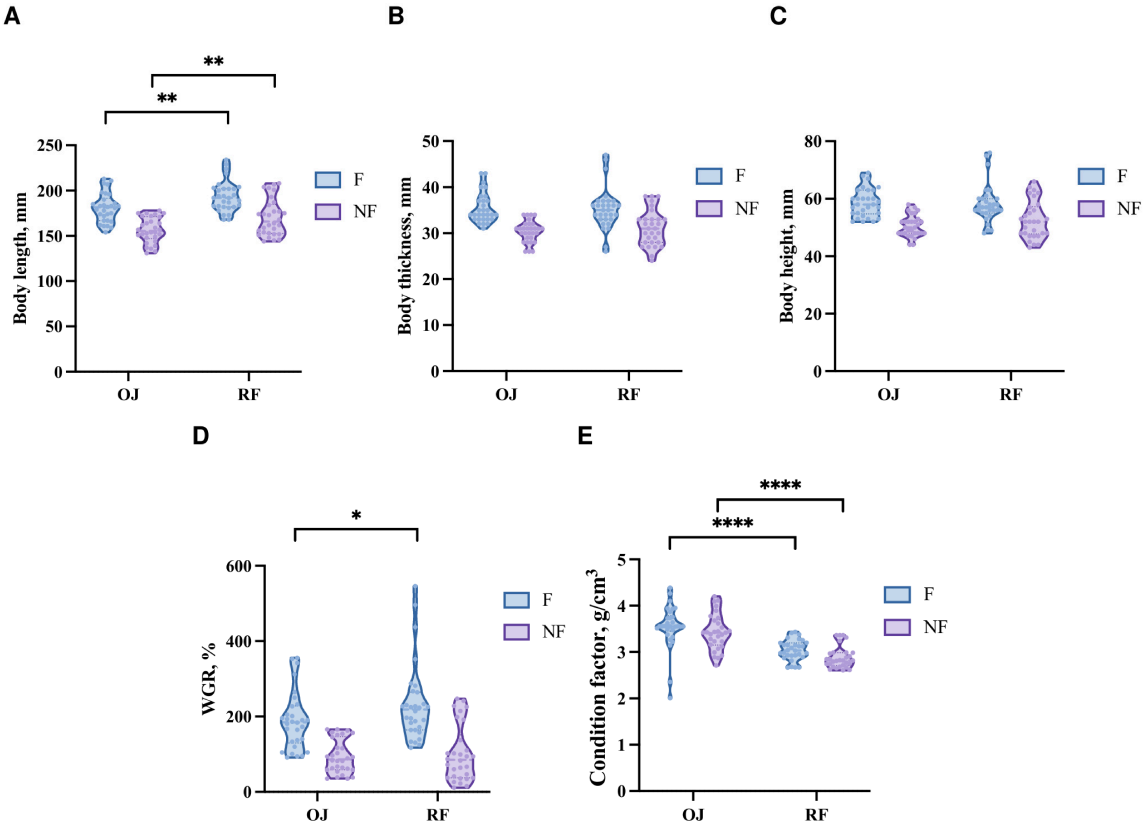


Figure 2. Growth performance of OJ and RF carp from F and NF paddy fields. (**A**) Body length; (**B**) Body thickness; (**C**) Body height; (**D**) Weight gain rate; (**E**) Body condition factor. Violin plots show the distribution of individual fish (n = 30 per variety per feeding treatment, i.e., 10 fish from each of three fields); dots are individual values. The feeding regime was applied at the field level, whereas both varieties were co-cultured in every field; all brackets therefore compare the two varieties within the same feeding treatment, i.e., within fields, which is the pre-planned contrast of interest and the only comparison treated as inferential. The two varieties were compared within each feeding treatment by Fisher's LSD following the two-way ANOVA; because the feeding regime was applied at the field level, the feeding term is not interpreted and no bracket is drawn for any between-field comparison. Only significant contrasts are bracketed. * $p < 0.05$, ** $p < 0.01$, **** $p < 0.0001$.

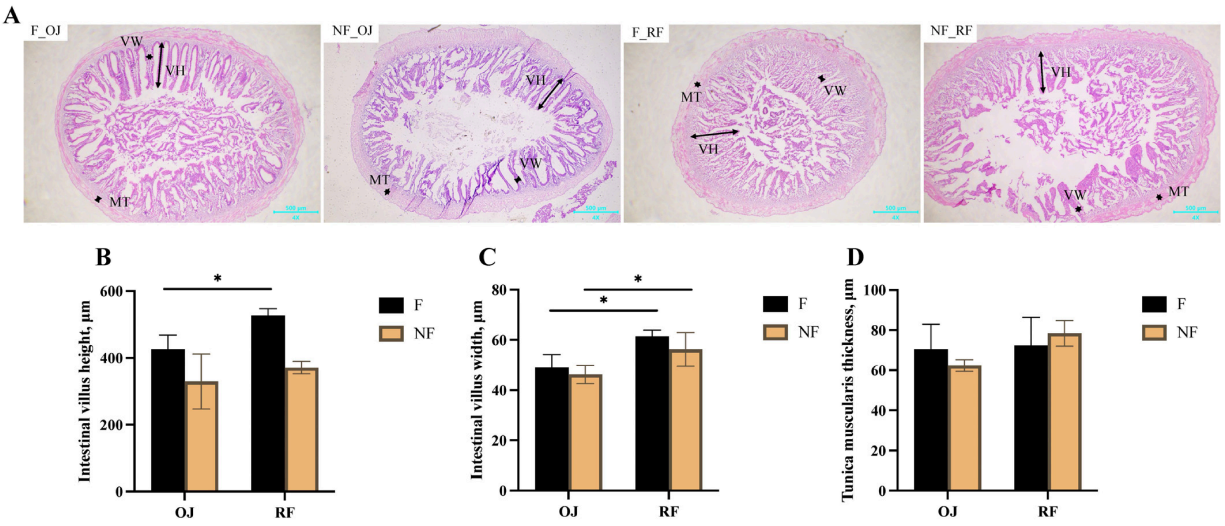


Figure 3. Intestinal morphological characteristics of OJ and RF carp under F and NF conditions. (**A**) Representative H&E-stained intestinal sections showing villus height (VH), villus width (VW), and tunica muscularis thickness (MT) (scale bar = 500 μm); (**B**) Intestinal villus height; (**C**) Intestinal villus width; (**D**) Tunica muscularis thickness. Fisher's LSD tests were performed after a two-way

ANOVA with feeding regime and variety as fixed factors, with the field mean as the unit of observation (n = 3 fields per feeding treatment; three fish per variety per field, 36 fish in total; three sections and 30 villi per fish; error bars are SD); as for growth traits, the feeding term is not interpreted and the variety contrast is made within fields. All brackets compare the two varieties within the same feeding treatment; no bracket is drawn for any between-field comparison. Only significant contrasts are bracketed. * $p < 0.05$.

3.3. Effects of Different Feeding Regimens on the Intestinal Microbial Community

Alpha diversity analysis indicated no appreciable differences in species evenness (Shannon index) of the gut microbiota between the two varieties or the two feeding strategies (Figure 4A). In contrast, species richness (Chao1 index) was higher in fish from the fed field than in those from the non-fed field for both OJ and RF carp (Figure 4B). PCoA showed that the first two principal coordinates (PCoA1 and PCoA2) explained 54.0% and 33.8% of the variation in community structure, respectively, with a cumulative contribution of 87.8%, adequately capturing ecological differences among samples (Figure 4C). Samples from different groups exhibited spatial separation that was not complete: the NF_RF and F_RF groups, as well as the NF_OJ and F_OJ groups, showed some dispersion; there was partial overlap between the NF_RF and NF_OJ groups, and a similar trend was observed between the F_RF and F_OJ groups. PERMANOVA based on Bray–Curtis dissimilarities showed that the intestinal communities differed significantly among the four groups (genus level: pseudo-F = 2.73, $R^2 = 0.506$, $p = 0.004$; species level: pseudo-F = 2.58, $R^2 = 0.492$, $p = 0.001$). In single-factor tests, feeding regime (confounded with field) explained 28.3% (genus) and 30.0% (species) of the total multivariate variation ($p = 0.003$ and 0.001), whereas carp variety explained only 12.4% (genus, $p = 0.215$) and 9.9% (species, $p = 0.343$) and was not a significant source of community-level variation; the variety × feeding interaction was also not significant ($R^2 = 0.099$ and 0.093; $p = 0.380$ and 0.369). Multivariate dispersion differed among groups (PERMDISP: $p = 0.003$ at the genus level and $p = 0.044$ at the species level), with fed groups being more heterogeneous than non-fed groups; the separation in Figure 4C therefore reflects within-group dispersion as well as group centroids and is not interpreted as evidence of functional superiority. With three individuals per group, the pairwise PERMANOVA contrasts (Table S5) have a minimum attainable p of 0.10. Rarefying all twelve samples to the smallest observed depth (205,276 reads) left the ordination essentially unchanged (r = 1.000 for PC1 across 20 replicates) and the four-group PERMANOVA remained significant in 60 of 60 replicates at each of four rarefaction depths; the compositional differences are therefore not an artefact of read number. Sequencing depth was nevertheless collinear with the feeding treatment, and PC1 correlated with depth both across samples (Spearman rho = −0.881, $p = 0.0002$) and within groups after centering (rho = −0.664, $p = 0.019$): the shallowest of the three fed RF libraries (226,000 reads) fell within the range of the non-fed samples, whereas the other two fed RF libraries did not. Because rarefaction does not reproduce this pattern, the cause lies in library preparation or DNA quality rather than in read number and cannot be removed post hoc.

At the phylum level, Proteobacteria dominated all samples (Figure 4D). *Uroviricota*, Firmicutes, Actinobacteria and Cyanobacteria were also detected, though at relatively low abundances. Further comparison revealed differences in the relative proportions of minor phyla among the groups. For instance, Firmicutes was the second most abundant phylum in the NF_OJ and NF_RF groups, whereas *Uroviricota* was more prominent in the F_OJ and F_RF groups. At the genus level, aside from unclassified taxa, the main genera included Pseudomonas, *Ralstonia* and *Clostridium* (Figure 4E). Clostridium was dominant in the NF_OJ and NF_RF groups. Aeromonas also exhibited relatively high abundance in the NF_OJ group, while Pseudomonas showed relatively high abundance in the NF_RF group. The F_OJ group displayed a distinct genus-level composition, with key identifiable

genera including *Enterovibrio*, *Vibrio*, *Carltongylesvirus*, etc. In contrast, *Pseudomonas* and *Ralstonia* were identified as the predominant genera in the F_RF group. At the species level (Figure 4F), among the major identifiable species, the dominant species in the NF_OJ group included uncultured *Caudovirales* phage, *Ralstonia pickettii*, *Aeromonas veronii* and *Acinetobacter bereziniae*. In the F_OJ group, the main dominant species were *Enterovibrio norvegicus*, *Escherichia virus* 4HA13, *Ralstonia pickettii*, *Erwinia virus Faunus*, etc. In the NF_RF group, dominant species consisted of uncultured *Caudovirales* phage, *Ralstonia pickettii*, the Pseudomonas fluorescens group, *Acinetobacter bereziniae*, etc. In the F_RF group, dominant species were uncultured *Caudovirales* phage, *Ralstonia pickettii*, *Aestuariivirga litoralis*, and the Pseudomonas fluorescens group.

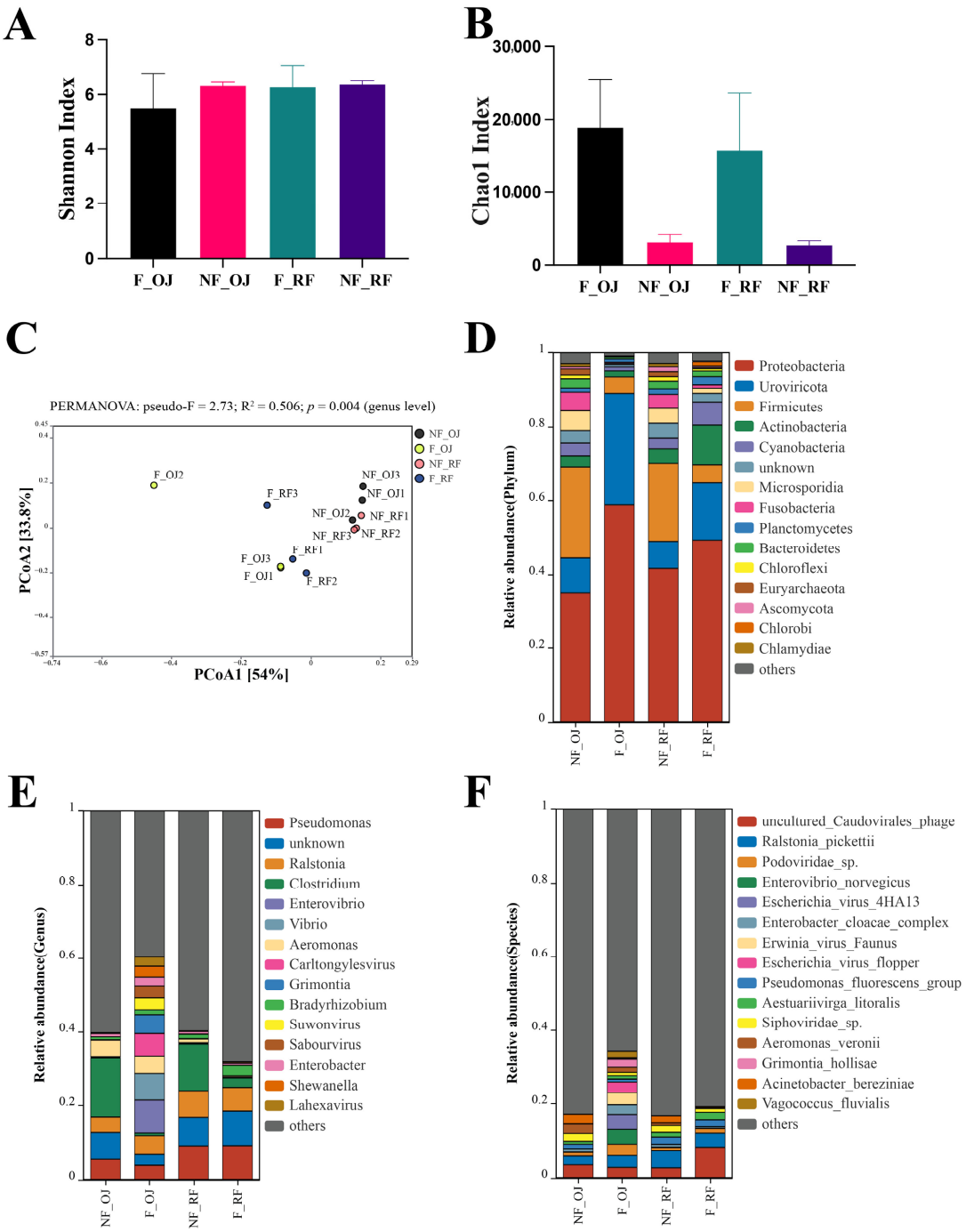


Figure 4. Diversity and composition of intestinal microbiota of OJ carp and RF carp in type F and NF rice–fish co-culture systems. (**A**) Alpha diversity of the intestinal microbiota assessed using the

Shannon index; (**B**) Alpha diversity of the intestinal microbiota assessed using the Chao1 index; (**C**) Beta diversity derived from PCoA analysis based on Bray–Curtis distances; PERMANOVA of the four groups was significant at both taxonomic levels (genus: pseudo-F = 2.73, R2 = 0.506, $p = 0.004$; species: pseudo-F = 2.58, $R^2 = 0.492$, $p = 0.001$; Table S5). (**D**–**F**) Relative abundance of the intestinal microbial communities at the phylum (**D**), genus (**E**), and species (**F**) levels; $n = 3$ per group, each sample being a pool of three fish from the same paddy field.

LEfSe analysis further revealed differential abundances of specific species between groups. Compared with the NF_OJ group, the F_OJ group showed a higher relative abundance of 25 species, including *Podoviridae* sp., *Cronobacter* phage vB CsaP GAP52, *Vibrio harveyi* group, *Salmonella* phage 7–11 and *Vibrio fluvialis*, and a lower relative abundance of 20 species, such as *Cetobacterium* sp. ZWU0022, *Clostridium pasteurianum*, *Lactococcus lactis*, *Cetobacterium* sp. ZOR0034 and *Clostridium acidisoli* (Figure 5A; Table S6). Comparing the F_RF group with the NF_RF group, the abundances of *Desulfurellales* bacterium, *Beijerinckiaceae* bacterium, and uncultured *Caudovirales* phage were higher, while those of *Acinetobacter bereziniae*, *Acidithiobacillus caldus* and *Clostridium acidisoli* were lower (Figure 5B; Table S6). In the comparison between the F_RF and F_OJ groups, 23 species had a lower relative abundance in the F_RF group, including *Cronobacter* phage vB CsaP GAP52, *Vibrio harveyi* group, *Salmonella* phage 7–11, *Aeromonas veronii* and *Vibrio fluvialis*, whereas only one species, *Vittaforma corneae*, had a higher relative abundance (Figure 5C; Table S6). Finally, comparing the two non-fed varieties, uncultured *Caudovirales* phage and *Acinetobacter bereziniae* were more abundant in the NF_OJ group, whereas *Ralstonia pickettii* and *Acidithiobacillus caldus* were more abundant in the NF_RF group (Figure 5D; Table S6).

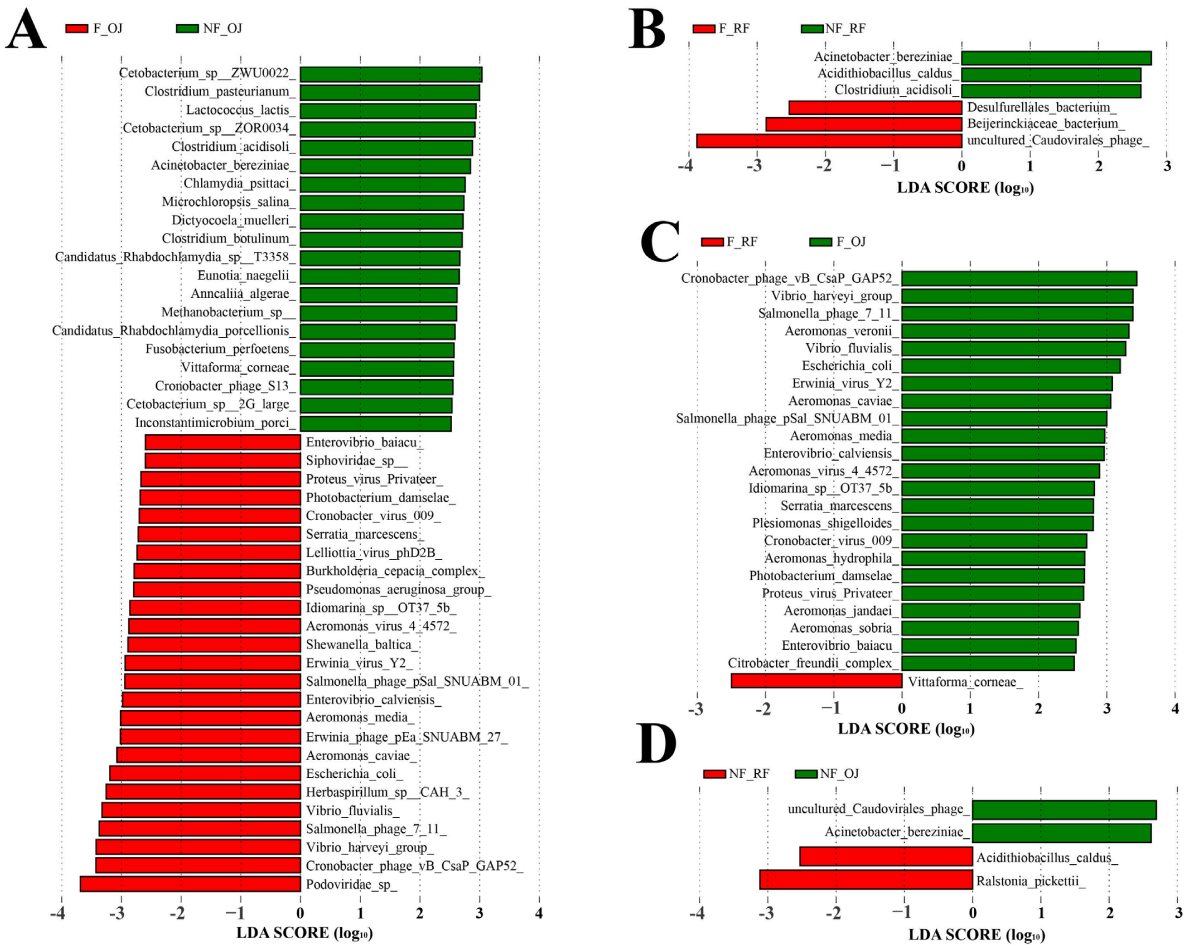


Figure 5. LEfSe analysis of the intestinal microbiota of OJ and RF carp in type F and NF rice–fish co-culture systems. LEfSe was used to identify differentially abundant taxa (LDA score > 2.5; $n = 3$;

no correction for multiple testing was applied) among groups: (**A**) F_OJ vs. NF_OJ and (**B**) F_RF vs. NF_RF, where these comparisons were made between different fields within the same variety; (**C**) F_RF vs. F_OJ and (**D**) NF_RF vs. NF_OJ, comparing the two varieties within fields under the same treatment.

3.4. Effects of Different Feeding Regimens on the Intestinal Microbial Function

Compared with the NF_OJ group, the F_OJ group exhibited higher relative abundance of 362 genes, including those encoding NADH dehydrogenase (ubiquinone) 1 alpha subcomplex subunit 2, stage V sporulation protein D (sporulation-specific penicillin-binding protein), rhomboid protease GluP, and spore germination protein KB. In addition, 421 genes, such as those encoding large subunit ribosomal protein L36, DNA transformation protein and related proteins, murein DD-endopeptidase, and type IV secretion system protein TrbC, exhibited lower relative abundances in the F_OJ group (Table S7). These gene sets were defined using a nominal $p < 0.05$, without correction for multiple comparisons. When Benjamini–Hochberg corrected values were applied, 276 of the 783 genes (109 higher, 167 lower) still had a corrected $p < 0.05$; 179 genes did not receive corrected values because they did not pass the independent screening criteria. Therefore, these gene lists are reported as candidate sets (Table S7). KEGG pathway enrichment analysis of these sets revealed enrichment in flagellar assembly, biofilm formation, the citric acid cycle (TCA cycle), cationic antimicrobial peptide (CAMP) resistance, and phosphotransferase system (PTS) pathways (Table S7). Similarly, compared with the NF_RF group, 90 genes exhibited higher relative abundance in the F_RF group, including genes encoding cystatin-A/B, iron-siderophore transport system permease protein, ACT domain-containing protein, and tRNA-intron endonuclease (archaea type). Additionally, 256 genes, such as those encoding pilus assembly protein Flp/PilA, DNA repair and recombination protein RAD52, putative endonuclease, and hydroxymethylglutaryl-CoA lyase, had lower relative abundance in the F_RF group (Table S8). Of these 346 genes, only 23 had adjusted $p < 0.05$. Enriched pathways included the cell cycle, fluorobenzoate degradation, DNA replication, flagellar assembly and the bacterial secretion system (Table S8). Because the enrichment analysis was based on metagenomic gene abundance, the identified pathways indicate functional potential only, rather than confirmed activity.

Under feeding conditions, 51 genes had a higher relative abundance in the F_OJ group than in the F_RF group, including those encoding large subunit ribosomal protein L36e, putative DeoR family transcriptional regulator stage III sporulation protein D, cyto-chrome-b5 reductase and large subunit ribosomal protein L8e; 554 genes had a lower relative abundance in the F_OJ group, such as those encoding N4-acetylcytidine amidohydrolase, anaerobilin synthase and type IV secretion system protein TrbH (Figure 6A; Table S9). Of these 605 genes, 75 retained an adjusted $p < 0.05$. KEGG enrichment indicated that the differences between the two varieties under feeding conditions were associated with flagellar assembly, biofilm formation, ubiquinone and other terpenoid-quinone biosynthesis, and the PTS and CAMP resistance pathways (Figure 6B; Table S9). Compared with the NF_RF group, the NF_OJ group had a higher relative abundance of 74 genes, including those encoding leader peptidase (prepilin peptidase)/N-methyltransferase, alpha-D-ribose 1-methylphosphonate 5-triphosphate synthase subunit PhnG and iron-sulfur cluster insertion protein, and a lower relative abundance of 90 genes, including those encoding 7-cyano-7-deazaguanine reductase, 4-amino-4-deoxychorismate lyase and protein PhnA (Figure 6C; Table S10). Notably, the genes with differential abundance between the two non-fed varieties were enriched in only one KEGG pathway, flagellar assembly (Figure 6D; Table S10); for this comparison none of the 164 genes retained an adjusted $p < 0.05$ (minimum adjusted $p = 0.116$).

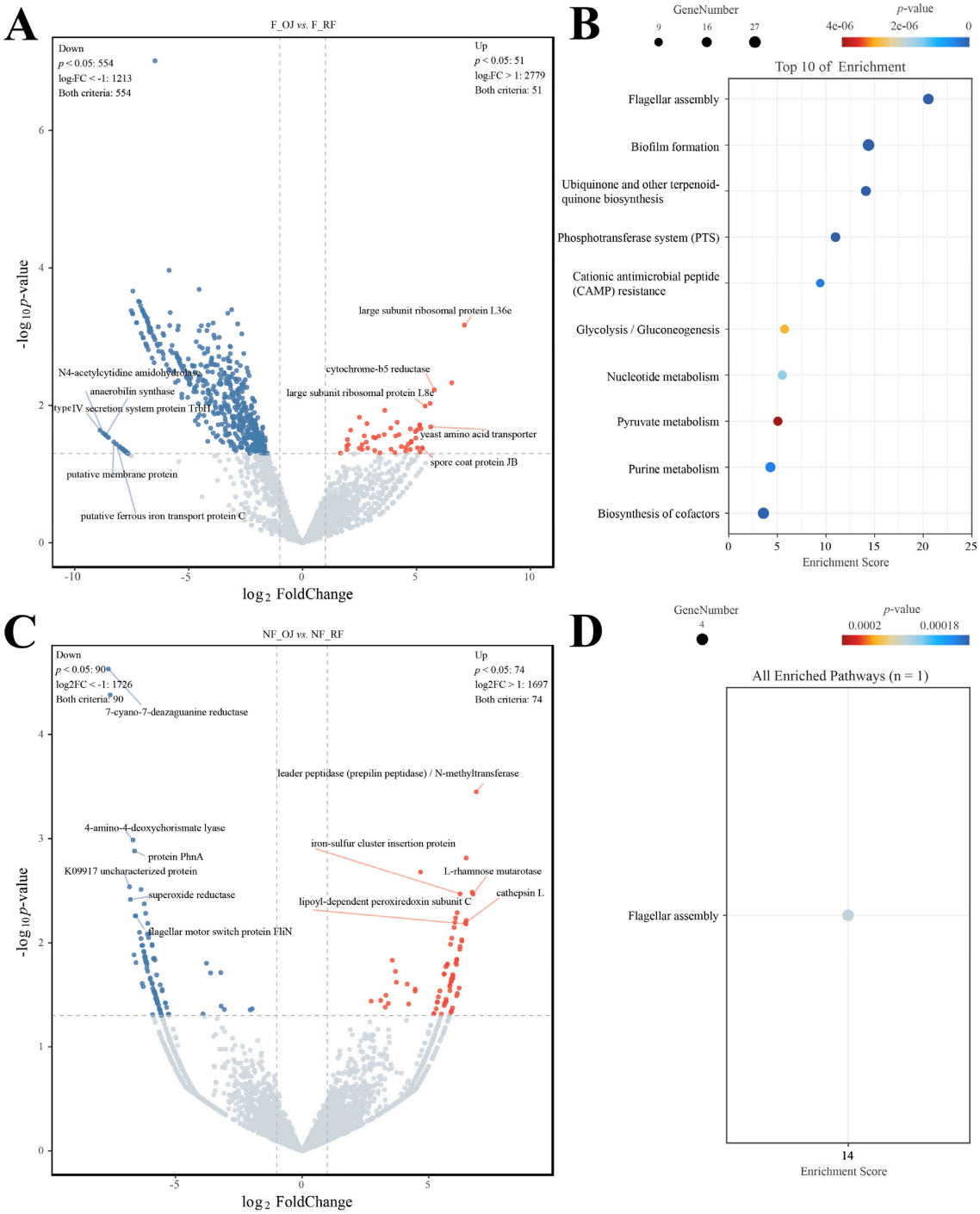


Figure 6. Results of the KEGG functional enrichment analysis of differentially abundant genes in the intestinal microbiota of OJ and RF carp under the F and NF rice–fish co-culture systems. (**A**,**C**) show volcano plots of gene abundance in the metagenome across different comparison groups: (**A**) F_OJ vs. F_RF, (**C**) NF_OJ vs. NF_RF. Red points represent genes with higher relative abundance ('More abundant'), blue points represent genes with lower relative abundance ("Less abundant") and grey points represent genes that do not meet either criterion. The two criteria are |log2(fold change)| > 1 and a nominal $p < 0.05$, applied without correction for multiple testing. In addition to the three coloured classes, each panel gives the number of genes with a nominal $p < 0.05$, the number with |log2(fold change)| > 1, and the number of genes that meet both criteria (labelled 'Both criteria'). (**B**,**D**) show KEGG functional enrichment analysis for the corresponding gene sets, displaying the most enriched pathways (those with a Benjamini–Hochberg adjusted $p < 0.05$ within the gene set tested; the number of pathways shown is given in the panel title). Dot size represents the number of genes in each term, and color (from blue to red) indicates the magnitude of enrichment.

3.5. Effects of Different Feeding Regimens on the Liver Metabolome of OJ and RF Carp

To explore the effects of rearing method on liver metabolism, we compared the four groups using PLS-DA with one predictive component on autoscaled data. The score plots showed a visual separation between the F_OJ and NF_OJ groups (PLS component 1: 33.8%; component 2: 23.9%; Figure S2A) and between the F_RF and NF_RF groups (28.7% and 20.2%; Figure S2C). However, model validation indicated that this separation was not predictive: R2Y was high (0.940–0.995), whereas Q2Y was ≤ 0.231 in all four comparisons and negative in two of them (F_OJ vs. NF_OJ: −0.083; F_RF vs. F_OJ: −0.720). In a permutation test over all 20 distinct two-group label assignments of six samples, the maximum R2Y obtained under random labeling reached 0.984–0.995, i.e., as high as the observed fit, and the minimum attainable permutation p was 0.10. These models are therefore not predictive, and the score plots are presented as exploratory visualizations rather than as evidence of group discrimination. Using the nominal criterion VIP ≥ 1 and $p < 0.05$, 69 metabolites were more abundant and 111 were less abundant in the F_OJ group than in the NF_OJ group, including 1,4-bis (2-ethylhexyl) sulfosuccinate, UDP-galactose and D-3-sulfolactaldehyde (more abundant) and floridimine, 4-hydroxyhexanoylcarnitine and 6-hydroxyoctanoylcarnitine (less abundant; Figure S2B; Table S11). Between the F_RF and NF_RF groups, 148 metabolites were more abundant and 52 were less abundant, including 3-phenyl-1H-pyrazole-4-carbaldehyde, lusitanicoside, and 6-methoxy-4-methylquinoline (more abundant) and S-acetylphosphopantetheine, inosinic acid and uric acid (less abundant; Figure S2D; Table S11). After Benjamini–Hochberg correction no metabolite remained significant in any of the four comparisons (minimum $q = 0.216$); these lists are therefore reported as hypothesis-generating candidates identified at a nominal $p < 0.05$.

We also evaluated the overall metabolic differences between the F_RF and F_OJ groups. PLS-DA showed a visual separation (PLS component 1: 29.3%; component 2: 29.1%; Figure S2E). There were 73 metabolites with differential abundance between these two groups, of which 43 were more abundant in F_OJ, including PC 15:0/20:2 (11Z, 14Z), (6Z)-hexadecenoylcarnitine and abacopterin A, and 30 were more abundant in F_RF, including tryptophan 2-C-mannoside, semilepidinoside B and 4′-hydroxyisolonchocarpin (Figure S2F; Table S11). The NF_OJ and NF_RF groups also showed visual separation (36.1% and 19.3%; Figure S2G). Further analysis identified 233 metabolites with differential abundance, of which 112 were more abundant in the NF_OJ group, including 3-O-acetylbotcineric acid, N-acetyl-L-aspartic acid and lusitanicoside, and 121 were more abundant in the NF_RF group, including UDP-galactose, S-acetylphosphopantetheine and retinoic acid (Figure S2H; Table S11). As in the other comparisons, no metabolite remained significant after Benjamini–Hochberg correction (minimum $q = 0.216$ across all four comparisons) and the PLS-DA models were not predictive (Q2Y ≤ 0.231); these lists are therefore reported as nominal, hypothesis-generating candidates.

3.6. Integrated Metagenomic and Metabolomic Analysis

As shown in Figure 7A, 17 pathways were enriched in the integrated analysis comparing the F_OJ and NF_OJ groups, primarily involving amino sugar and nucleotide sugar metabolism, purine metabolism and pyrimidine metabolism (Table S12). A total of 487 positive correlations were identified (Figure 7B; Table S12), 191 of which remained significant after Benjamini–Hochberg correction applied within each gene across the microorganisms tested for it. Genome-based linkage indicated that *Photobacterium damselae* carries genes annotated to purine metabolism (K00759, K08722, K00951), pyrimidine metabolism (K08722), and galactose metabolism (K01190), which are consistent with the formation of adenosine, thymidine, and UDP-galactose, respectively; *Aeromonas media* carries genes annotated to purine metabolism (K00759, K01525, K08722), glutathione metabolism (K01919, K01256),

and arginine and proline metabolism (K01585), which are consistent with the formation of adenosine, L-ornithine, and 4-acetamidobutanoate (Figure 7C). In addition, 20 intestinal microorganisms, including *Aeromonas caviae*, *Burkholderia cepacia* complex, and *Escherichia coli*, were linked to 11 metabolites with differential abundance, such as adenosine, L-ornithine, and oxoadipic acid, in OJ carp under both conditions (Figure 7C; Table S11). These relationships are correlative and are presented as candidate functional links rather than as evidence that the intestinal microbiota regulates host metabolism.

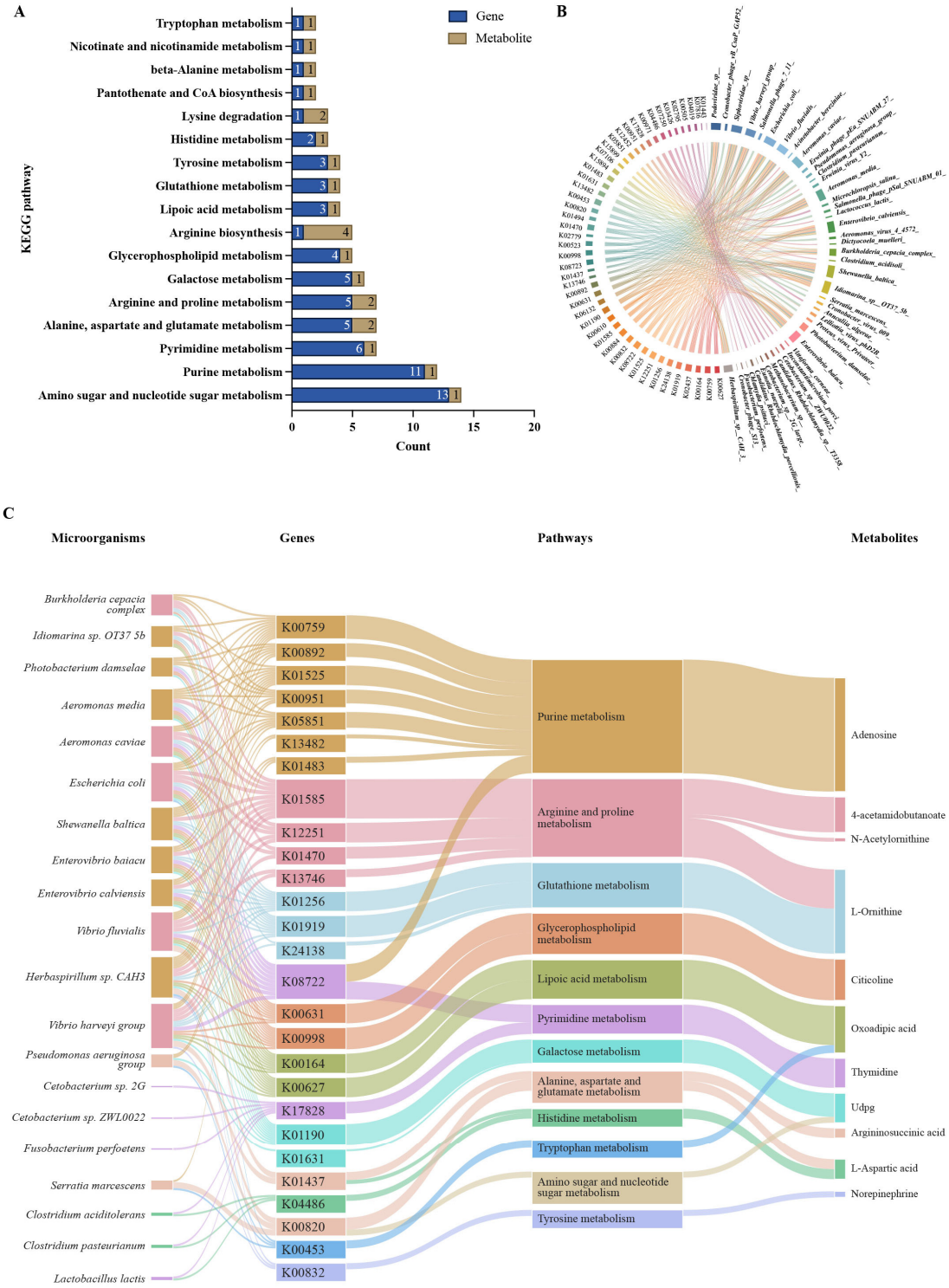


Figure 7. Integrated analysis of genes with differential abundance, metabolites with differential abundance and microorganisms with differential abundance in OJ carp under F and NF conditions.

(**A**) Co-enrichment analysis of KEGG pathways for genes with differential abundance in intestinal contents and liver metabolites; (**B**) positive correlations between microorganisms with differential abundance and genes with differential abundance in intestinal contents; (**C**) network analysis of associations among microorganisms, genes and metabolites with differential abundance. $n = 3$ per group, with each group representing fish sampled from different fields under the same feeding regime. The correlations shown are positive correlations with a nominal $p < 0.05$, and the corresponding Benjamini–Hochberg adjusted p values are reported for all pairs tested in Table S12. Genes are identified by KO identifiers; the corresponding gene descriptions and EC numbers are given in Table S7.

A comparison of F_RF and NF_RF identified 22 enriched pathways, primarily involving purine metabolism, arginine biosynthesis and amino sugar and nucleotide sugar metabolism (Figure 8A; Table S13), and revealed 44 positive correlations (Figure 8B; Table S13), 32 of which remained significant after the same correction. Genome-based linkage indicated that a bacterium of the family Beijerinckiaceae carries genes annotated to arginine and proline metabolism (K01470) and to phenylalanine, tyrosine and tryptophan biosynthesis (K04518), consistent with the formation of L-ornithine, L-arginine and L-phenylalanine; bacteria of the order Desulfurellales carry an aspartate 1-decarboxylase gene (K01579) linked to β-alanine metabolism and to pantothenic acid and coenzyme A biosynthesis, consistent with the formation of L-aspartate; and *Clostridium acidisoli* and *Acinetobacter bereziniae* carry genes annotated to amino sugar and nucleotide sugar metabolism (K01443), consistent with the formation of UDP-galactose, uridine 5′-diphosphoglucuronic acid and N-acetyl-D-galactosamine (Figure 8C; Table S13).

A comparison of F_OJ and F_RF revealed three enriched pathways: purine metabolism; alanine, aspartate and glutamate metabolism; and arginine biosynthesis (Figure S3A; Table S14). Correlation analysis identified 100 positive correlations (Figure S3B; Table S14), 34 of which remained significant after the same correction. Genome-based linkage indicated that *Aeromonas hydrophila* carries genes annotated to purine metabolism (K00526, K00951), and to alanine, aspartate, and glutamate metabolism (K01424, K14260), and arginine biosynthesis (K14260), consistent with the formation of uric acid and argininosuccinate. Sixteen intestinal microorganisms, including *Aeromonas jandaei*, *Aeromonas veronii*, *Aeromonas sobria* and *Enterovibrio calviensis*, were linked to both argininosuccinate and uric acid in OJ and RF carp under fed conditions (Figure S3C; Table S13).

Ten pathways were enriched in the comparison between NF_OJ and NF_RF, primarily involving purine metabolism, amino sugar and nucleotide sugar metabolism, and riboflavin metabolism (Figure S4A; Table S15). Correlation analysis identified eight positive correlations (Figure S4B; Table S15), one of which remained significant after the same correction. Among the eight correlations, the N-carbamoylputrescine amidase (K12251) of Acidithiobacillus caldus maps to arginine and proline metabolism and is co-located with the detection of spermine and spermidine. The FMN reductase (K00299) of Ralstonia pickettii maps to riboflavin metabolism and is co-located with the detection of riboflavin (Figure S4C; Table S15). These are associations between an annotated gene function and the presence of a metabolite in the same sample group; the dataset contains no transcription, expression or isotope-labelling evidence, and the analysis therefore does not show that these taxa produce or regulate these metabolites.

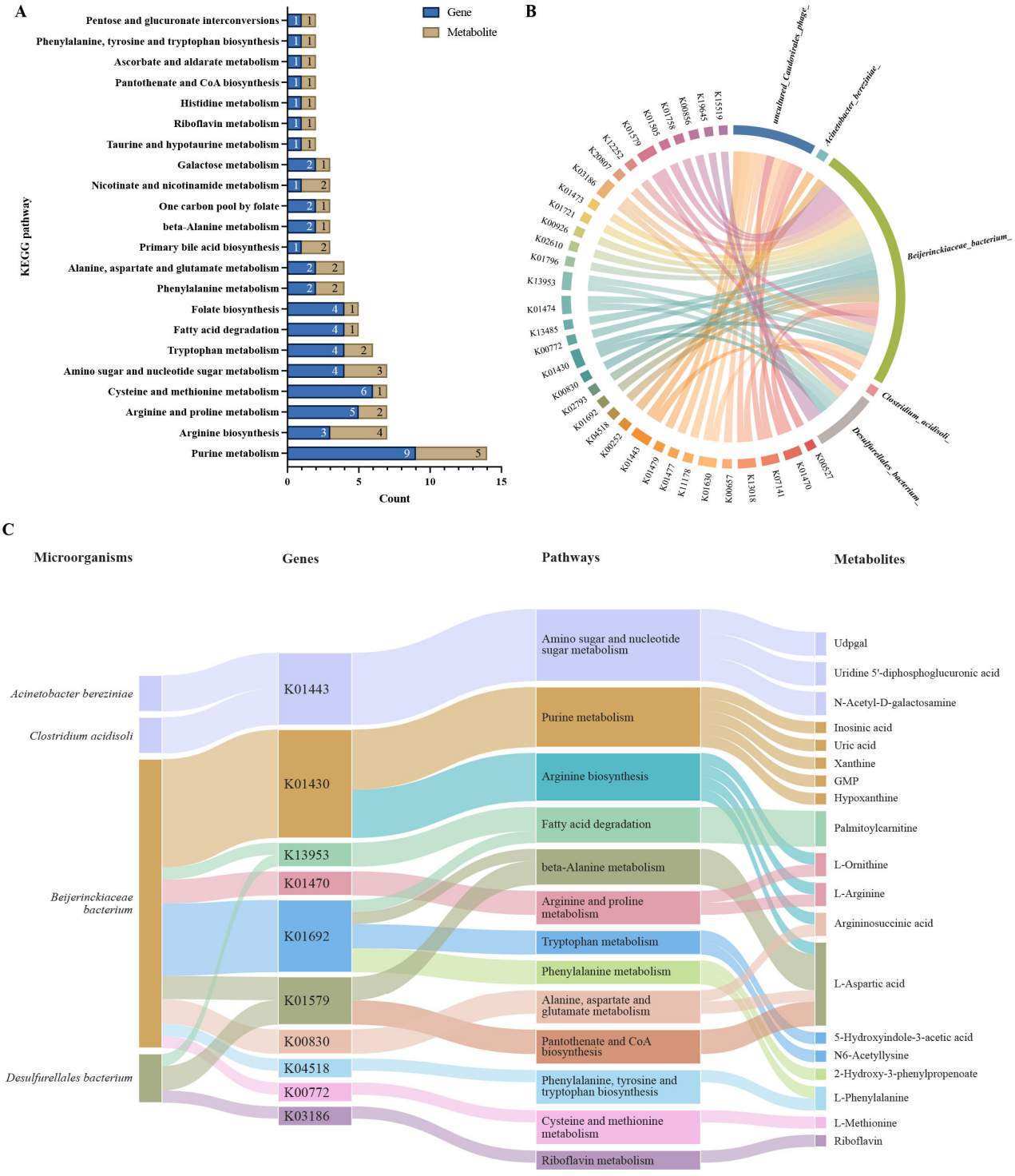


Figure 8. Results of a comprehensive analysis of genes with differential abundance, metabolites with differential abundance and microorganisms with differential abundance in RF carp under two feeding conditions. (**A**) Co-enrichment analysis of KEGG pathways between genes with differential abundance in intestinal contents and liver metabolites; (**B**) positive correlations between microorganisms with differential abundance and genes with differential abundance; (**C**) network analysis of associations among microorganisms, genes, and metabolites with differential abundance. $n = 3$ per group, with each group representing fish sampled from different fields under the same feeding regime. All correlations shown are positive; nominal $p < 0.05$; and the corresponding Benjamini–Hochberg adjusted p values are reported for all pairs tested in Table S13. Genes are identified by KO identifiers; the corresponding gene descriptions and EC numbers are given in Table S8.

4. Discussion

As an ecologically green farming model, rice–fish co-culture has been recognized as a "Globally Important Agricultural Heritage System" (GIAHS), with advantages reflected in improved rice and fish quality, enhanced overall benefits of paddy fields, and sustainable development of the aquaculture industry and environment [11]. Different farming models and management practices can lead to variations in fish growth performance, muscle quality and nutrition, intestinal microbiota, host metabolism, and even stress resistance [23]. This study evaluated the environmental microbial community, growth performance, intestinal microbial composition and function, and liver metabolic profile of two common carp varieties reared under fed and non-fed conditions in a rice–fish co-culture system. A combined metagenomic and metabolomic analysis was used to explore potential functional relationships between the intestinal microbiota and host metabolism.

4.1. Impact of Feeding Regimens on Environmental Microbial Communities

The study found that, although there were no appreciable differences in the α-diversity of microbial communities in water and sediments in the experimental fields under the two management strategies, these communities appeared to be separated in ordination space. Because the community-level tests did not reach significance and the LEfSe analysis was uncorrected, the taxa discussed here are treated as descriptive indicators of habitat conditions rather than as evidence of a feeding effect. In the NF group, typical oligotrophic freshwater bacteria were observed, including *Flavobacterium aciduliphilum*, *Novosphingobium*, *Sphingomonadaceae*, and *Methylophilaceae*. *Flavobacterium aciduliphilum* was originally isolated and described from a freshwater environment [24]; both *Novosphingobium* and *Sphingomonadaceae* belong to the family *Sphingomonadaceae*, a group of bacteria with strong tolerance to nutrient fluctuations and starvation stress, commonly native to oligotrophic freshwater environments [25]. In the F group, *Sphingobacterium* was detected, which is commonly found in organic matter-rich environments and has strong organic matter-degrading capacity [26]. Additionally, nitrogen fertilizer application can drive changes in soil fungal community structure in rice–fish systems, with total nitrogen and available nitrogen serving as key factors [27]. In this study, the fields that received feed also received an additional input of organic matter, which may be associated with the reorganization of microbial community structure by altering nutrient levels in the water and sediment. Notably, the enrichment of *Aurantimicrobium* in the water of the feeding group may be associated with the increased availability of easily degradable organic matter in the feed, while the reduction in specific taxa (e.g., RBG-13-54-9) in the sediment suggests competitive inhibition of benthic microbial niches in the fed fields [14]. These findings suggest that feed supplementation is associated with the restructuring of environmental microbial communities in rice–fish systems and that benthic community composition differs among plots under the two management strategies.

4.2. Impact of Feeding Regimens on Fish Growth and Intestinal Morphology

Rice–fish co-culture not only maintains rice yields while reducing chemical inputs but also provides additional fish production [28]. Fish sampled from the fed fields were larger and had higher WGR than those from the non-fed fields, although this difference cannot be attributed to feeding alone because feeding was confounded with field identity. Body length, a directly measured trait, was greater in RF than in OJ carp in both the fed and non-fed fields, indicating that the two varieties differ in growth performance when reared under identical conditions. OJ carp maintained a certain level of growth under NF conditions, which may be related to their genetic adaptations to long-term paddy field environments. Previous studies have shown that, Qingtian field carp (PF-carp), as a core species in the GIAHS, has developed high genetic diversity and multiple body color types

through millennia of domestication, with morphological features (e.g., caudal fin, dorsal fin) that differ significantly from those of common carp [29]. The OJ carp in this study is a type of PF-carp, whereas RF carp is a selectively bred variety; the two therefore differ in genetic background, which may contribute to the observed growth difference, although feed utilization was not quantified. This is consistent with the observation that the villus height of RF carp in the fed group was greater than that of OJ carp, indicating a larger intestinal absorption area. Furthermore, the villus height of fish in the fed group was higher than that of fish in the unfed group, consistent with the physiological expectation that "improved nutritional status promotes intestinal epithelial proliferation."

4.3. Impact of Feeding Regimens on Intestinal Microbial Composition and Function

Alterations in intestinal microbial composition and function serve as a key bridge linking feeding strategies to host metabolism. Fish from the fed fields showed higher intestinal species richness (Chao1 index) than those from the non-fed fields, whereas evenness (Shannon index) did not differ; because sequencing depth was collinear with the feeding treatment (Section 3.3), this richness difference is reported as an observation and not as a feeding effect. In the NF group, Firmicutes (e.g., *Clostridium*) exhibited higher abundance, whereas Uroviricota (a viral phylum) was more prominent in the F group, suggesting that host-microbe-virus interactions may differ between the fed and non-fed fields. Notably, the F group contained more virus-related sequences (e.g., *Caudovirales* phages), while beneficial bacteria such as *Cetobacterium* were less abundant. *Cetobacterium* is a key genus for short-chain fatty acid (SCFA) production in fish intestines. Its lower relative abundance in the fish sampled from the fed fields is consistent with, but does not demonstrate, a difference in intestinal fermentation: SCFA concentrations were not measured in this study, and the observation rests on the relative sequence abundance of one potential producer only. These findings are consistent with other studies reporting that, compared with traditional pond aquaculture, the intestinal microbiota of carp in rice–fish systems contains a lower relative abundance of sequences assigned to taxa that include known pathogens, and has been reported to support higher SCFA production [27,30,31]. In addition, in the F group the intestinal microbiota of OJ carp showed a higher relative abundance of several taxa, including *Aeromonas veronii* and members of the *Vibrio harveyi* group, than that of RF carp. Some strains assigned to these taxa are described as pathogens of aquatic animals [32,33], but this dataset provides relative sequence abundance only, with no virulence assay, no measurement of virulence-gene expression and no clinical, gross-pathological or histopathological evidence of disease. These sequences therefore cannot be interpreted as infection, virulence or disease risk. Sequences of *Salmonella* phage 7–11 were also more abundant in the OJ carp intestine. Bacteriophages are abundant in aquatic environments and phage cocktails have been investigated for the control of *Salmonella* ex vivo [34]; however, sequences of this kind report the presence of phage DNA only, provide no evidence for the presence, abundance or activity of *Salmonella* itself, and this observation is therefore descriptive.

Two features of the taxonomic assignments require caution. First, Vibrio harveyi is a marine organism and cannot be assumed to colonise a freshwater paddy-field system. In our data the taxa with marine affinities—*Vibrio*, *Enterovibrio* (*E. norvegicus*), and *Photobacterium damselae* were detected essentially only in fish sampled from the fed fields and were absent or rare in the non-fed fields, although all six fields were adjacent and shared the same water source. The most parsimonious explanation is that these sequences entered with the supplemental feed, a commercial pellet that contains fish meal and is therefore a plausible vehicle for marine-associated taxa, rather than that they represent an established component of the carp gut community, and they are no longer discussed as intestinal pathogens. Second,

all taxonomic assignments derive from 150 bp paired-end short reads annotated against a reference database. Such assignments are reasonably reliable at genus level but frequently unreliable at species level, and our own data illustrate this: Table S6 lists *Vibrio cholerae*, Clostridium botulinum, Streptococcus agalactiae and *Streptococcus pneumoniae* among the differentially abundant species, and *V. harveyi* is reported as the *Vibrio harveyi* group. *V. cholerae* and *C. botulinum* are implausible in this environment and were not confirmed by any independent method, so their appearance reflects misassignment of short reads to the closest reference genome rather than true presence. Species-level names in this work are therefore reported as sequences assigned to the named taxon, and no species-level identification is used to support any functional or pathological inference.

At the functional level, in the comparison of F_OJ and NF_OJ, genes with higher relative abundance were annotated to NADH dehydrogenase subunits and spore formation proteins, whereas genes with lower relative abundance included those for ribosomal proteins and DNA transformation proteins. KEGG enrichment indicated enrichment of flagellar assembly, biofilm formation, the TCA cycle, CAMP resistance and the PTS. Similarly, in the F_RF vs. NF_RF comparison, genes encoding cystatin and siderophore transporters had a higher relative abundance, whereas those for fimbrial assembly proteins and DNA repair/recombination proteins had lower relative abundance, with enrichment of the cell cycle, fluorobenzoate degradation, DNA replication, flagellar assembly and the bacterial secretion system. Because these analyses are based on gene abundance in the metagenome, they describe the functional potential of the community rather than its realized activity. In particular, the enrichment of flagellar assembly and biofilm formation pathways may be associated with enhanced motility and adhesion in a high-nutrient environment, consistent with previous observations that feed input alters microbial community structure and interactions [35]. The inter-variety comparison further showed that, under the same feeding management, the gene sets with differential abundance differed between OJ and RF carp. In OJ carp, the genes with higher relative abundance were annotated mainly to ribosomal proteins. Those with a lower relative abundance included the type IV secretion system and GntR family transcriptional regulators, with enrichment of flagellar assembly and biofilm formation. This pattern may be associated with the contrasting domestication histories of the two varieties: Qingtian field carp have been domesticated for millennia and retain high genetic diversity and distinctive morphological features [29], and OJ carp, as one such variety, may reflect this adaptive evolution in the functional composition of its intestinal microbiota.

4.4. Impact of Feeding Management on the Liver Metabolome

Liver metabolomics analysis revealed nominal differences in the metabolic profiles of the two varieties under different feeding strategies. In the comparison between F_OJ and NF_OJ, metabolites that were less abundant in F_OJ included 6-hydroxyoctanoylcarnitine and adenosine, whereas those that were more abundant included UDP-galactose and lecithin. In F_RF vs. NF_RF, metabolites that were more abundant in F_RF included 3-phenyl-1H-pyrazole-4-carbaldehyde and N′-formylkynurenine, whereas those that were less abundant included S-acetylphosphopantetheine and inosine monophosphate. These metabolites participate in pathways such as energy metabolism, lipid metabolism, amino acid metabolism, and nucleotide metabolism, suggesting that a broad association between nutritional status and fish liver metabolism. In a previous study on the high-temperature adaptation of PF-carp, the hepatopancreas did not show tissue damage or oxidative stress under 34 °C stress, but the endoplasmic reticulum protein processing pathway was significantly activated, with elevated expression of HSP40, HSP70, and HSP90 proteins [36]. The metabolomic differences observed between the two strategies may be associated with

differences in nutritional status and environmental differences between the fed and non-fed fields, which were not monitored in this study; they cannot be attributed to any single factor. Notably, the lower abundance of adenosine in the fed fields may be associated with the intestinal microbiota through purine metabolism, whereas the higher abundance of UDP-galactose may suggest an adjustment in carbohydrate metabolism pathways.

4.5. Integrated Metagenomic and Metabolomic Analysis Reveals Intestinal Microbiota-Host Metabolic Interactions

In OJ carp, two taxa carry genes annotated to purine metabolism, glutathione metabolism and galactose metabolism that are consistent with the formation of adenosine, ornithine and cytidine diphosphate choline: *Aeromonas media*, and *Photobacterium damselae*, which was detected essentially only in fish from the fed fields and is attributed to the supplemental feed rather than to the resident gut community. In RF carp, *Beijerinckiaceae bacterium* and *Desulfurellales bacterium* carry genes linked to L-ornithine, L-arginine, and 5-hydroxyindoleacetic acid through arginine biosynthesis, fatty acid degradation, and tryptophan metabolism. These results indicate associations between intestinal taxa and host metabolites; they do not demonstrate that the intestinal microbiota regulates host metabolism, and they are consistent with previous findings that rice–fish systems enhance carp intestinal microbial diversity and beneficial metabolite production relative to traditional pond aquaculture [27,31]. Under feeding conditions, *Aeromonas hydrophila* and the *Vibrio harveyi* group, the latter likewise attributed to the feed, carry genes consistent with the formation of uric acid and argininosuccinate through purine metabolism, alanine/aspartate/glutamate metabolism and arginine biosynthesis, and these gene sets differed between the OJ and RF varieties. Uric acid, as the product of purine metabolism, may be associated with degradation of nucleic acids from feed by the intestinal microbiota, while argininosuccinate, a key intermediate in the urea cycle, may be associated with active protein metabolism. Under non-feeding conditions, *Acidithiobacillus caldus* and *Ralstonia pickettii* carry genes linked to spermine, spermidine, and riboflavin through arginine/proline metabolism and riboflavin metabolism, respectively, suggesting that in a low-nutrient environment these taxa may be associated with polyamine and vitamin metabolism in the host.

4.6. Limitations

The following limitations should be considered. First, the sample size for the high-throughput analysis was small (three samples per group, each a pool of three fish from the same paddy field); therefore, the omics results should be regarded as hypothesis-generating: the PLS-DA model for liver metabolomics did not pass cross-validation, and after Benjamini–Hochberg correction, no metabolites remained statistically significant. The LEfSe biomarker analysis was not corrected for multiple comparisons; therefore, its *p*-values are nominal, and the resulting rankings are purely descriptive. Second, although this experimental design can establish associations between the gut microbiota and the host metabolome, it cannot establish causality. Third, this experiment did not include field-level water chemistry (dissolved inorganic nitrogen and phosphorus, organic loading, chlorophyll a, or the biomass of natural food organisms), feeding rates, total feed intake, feed conversion ratios, or nutrient inputs, nor did it include an economic analysis. Water chemistry was not part of the original sampling protocol, which was designed around fish performance and the microbiome rather than around environmental characterisation; consequently, the larger body size and taller villi of fish sampled from the fed fields may in part reflect a higher availability of natural food rather than the feed itself, and the discussion of feed efficiency and economic benefits lacks support from these data. In addition, sequencing depth differed systematically between fed and non-fed fields and was collinear with the

treatment; although rarefaction showed that the compositional estimates are insensitive to read number, this collinearity provides a further and independent reason why all between-field comparisons are reported descriptively. No clinical, gross-pathology, bacteriological or parasitological data were collected, so the sequence-based observations reported here cannot be read as evidence of infection or disease. Future studies should incorporate controlled tank or sterile experiments using specific microbial communities to test feeding effects and the mechanistic roles of specific taxonomic groups. Finally, intestinal tissues were fixed in 4% neutral paraformaldehyde, which is adequate for routine H&E morphometry but preserves the mucus layer and fine epithelial detail less well than Bouin's or Carnoy's solution; the histological conclusions are therefore restricted to villus height, villus width and tunica muscularis thickness.

5. Conclusions

This study compared the growth, intestinal microbiota, and liver metabolism of two common carp varieties co-cultured in the same rice–fish integrated farming system under both fed and unfed conditions. Significant differences were observed between the two strains in multiple aspects: under both rearing strategies, RF carp had greater body length than OJ carp, and RF carp also had wider intestinal villi in both the fed and non-fed fields; conversely, OJ carp had a higher condition factor. However, weight gain rate did not differ consistently between the strains: the variety effect across both feeding treatments was not significant ($p = 0.081$), although RF carp grew faster than OJ carp within the fed fields ($p = 0.033$). The intestinal microbiota, metagenomic functions and liver metabolome also showed differences between varieties that we treat as candidate signals. Fish sampled from the fed fields grew faster and had taller intestinal villi and a higher species richness (Chao1) than those from the non-fed fields, although in this dataset richness cannot be separated from the systematic difference in sequencing depth between the two field types. Based on genomic annotation and correlation, a comprehensive analysis revealed associations between gut taxonomic groups and host metabolites, for example, between Photobacterium damselae and adenosine; between Beijerinckiaceae bacterium and L-ornithine and L-arginine; and between Aeromonas hydrophila and uric acid and argininosuccinate, laying the foundation for subsequent in-depth experimental validation. Because both analyses rest on three field-level replicates per group (three fish of the same variety pooled per field), and because no metabolite remained significant after Benjamini–Hochberg correction (minimum $q = 0.216$ across all four comparisons) and the liver PLS-DA models were not predictive (Q2Y ≤ 0.231, negative in two of the four comparisons), the functional and metabolic findings reported here are exploratory and are intended to generate hypotheses rather than to establish differences between varieties or feeding regimes. Taken together, the growth and intestinal morphology results indicate that under identical rice–fish co-culture conditions, the responses of these two varieties differ; the omics profiles are consistent with this pattern but remain exploratory, and these observations can serve as a reference for developing feeding regimens tailored to different varieties in rice–fish systems.

Supplementary Materials: The following supporting information can be downloaded at: https://www.mdpi.com/article/10.3390/microorganisms14122756/s1, Figure S1: Differences in the diversity and composition of sedimentary microbial communities in type F and NF rice-fish co-culture systems. Figure S2: Metabolomic analysis profiles of OJ and RF carp under the F and NF rearing conditions. Figure S3: Integrated analysis of genes with differential abundance, metabolites with differential abundance and microorganisms with differential abundance in OJ and RF carp under the F condition (F_OJ vs. F_RF). Figure S4. Integrated analysis of genes with differential abundance, metabolites with differential abundance and microorganisms with differential abundance in OJ and RF carp under the NF condition (NF_OJ vs. NF_RF). Table S1: Sequencing quality statistics for the 12 intestinal

metagenome samples analysed in this study. Table S2: PERMANOVA (exact permutation) and PERMDISP results for the water and sediment bacterial communities (OTU and family level), together with sensitivity analyses of the same comparisons under rarefaction, presence/absence transformation and Hellinger transformation. Table S3: LEfSe analysis results for indicator groups in water and sediments from the F and NF fields. Table S4: Survival of Oujiang color carp (OJ) and FFRC No. 2 red carp (RF) in each of the six paddy fields over the 64-day co-culture experiment. Table S5: PERMANOVA and PERMDISP results for the intestinal metagenomic communities (genus and species level): four-group model, single-factor models, two-factor model, and all pairwise contrasts computed by exact permutation. Table S6: LEfSe analysis results for species with abundance differences between different comparison groups. Table S7: Results of the analysis of genes with differential abundance and KEGG pathway enrichment between the F_OJ group and the NF_OJ group. Table S8: Results of the analysis of genes with differential abundance and KEGG pathway enrichment between the F_RF group and the NF_RF group. Table S9: Results of the analysis of genes with differential abundance and KEGG pathway enrichment between the F_OJ group and the F_RF group. Table S10: Results of the analysis of genes with differential abundance and KEGG pathway enrichment between the NF_OJ group and the NF_RF group. Table S11: Analysis results for metabolites that differed between the various comparison groups. Table S12: Information on the association analysis of genes with differential abundance, metabolites, and microorganisms between the F_OJ and NF_OJ groups. Table S13: Information on the association analysis of genes with differential abundance, metabolites, and microorganisms between the F_RF and NF_RF groups. Table S14: Information on the association analysis of genes with differential abundance, metabolites, and microorganisms between the F_OJ and F_RF groups. Table S15: Information on the association analysis of genes with differential abundance, metabolites, and microorganisms between the NF_OJ and NF_RF groups.

Author Contributions: Conceptualization, W.Z. and Z.D.; methodology, M.L.; validation, Y.J.; formal analysis, M.L. and J.F.; investigation, M.L. and Y.J.; resources, M.Q.; data curation, L.W.; writing—original draft preparation, M.L.; writing—review and editing, W.Z. and Z.D.; supervision, Z.D.; funding acquisition, M.L. and W.Z. All authors have read and agreed to the published version of the manuscript.

Funding: This research was funded by the National Key Research and Development Project (2023YFD2400204); Central Public Interest Scientific Institution Basal Research Fund, CAFS (2025JBFM05); Zhejiang Provincial Science and Technology Collaboration Project (2025SNJF087) and Science and Technology Program of Xinjiang Uyghur Autonomous Region (2024E02021).

Institutional Review Board Statement: The study was approved by the Animal Care and Use Committee of the Freshwater Fisheries Research Center (FFRC), Chinese Academy of Fishery Sciences (CAFS) (approval No. ACUC-FFRC-2024-04-03, April 2024; experimental period April 2024-December 2025) and conducted in accordance with the committee recommendations (BC2013863, 9/2013) and the guidelines and regulations issued by the Ministry of Science and Technology, Beijing, China (No. 398, 2006).

Informed Consent Statement: Not applicable.

Data Availability Statement: The original contributions presented in the study are publicly available. The raw sequencing data of metagenomic have been deposited in the NCBI Sequence Read Archive (SRA) under the accession number PRJNA1506383. Liver metabolomics data have been uploaded to the MetaboLights database (accession number MTBLS15304). Water and sediment 16S rRNA amplicon sequences have been deposited in the NCBI Sequence Read Archive under the accession number PRJNA1559816. Sample identifiers were renamed in this revision to make the experimental unit explicit; the identifiers under which the data were deposited are those of the original submission and are retained in the repository records, and their correspondence to the identifiers used here is available from the corresponding author.

Acknowledgments: We thank Nanjing Genepioneer Biotechnology Co., Ltd. (Nanjing, China) for their assistance in the sample sequencing process.

Conflicts of Interest: The authors declare no conflicts of interest.

Abbreviations

The following abbreviations are used in this manuscript:

WGR	Weight Gain Rate
KEGG	Kyoto Encyclopedia of Genes and Genomes
UHPLC	Ultra-high-performance Liquid Chromatography
IDA	Information-dependent Acquisition
GIAHS	Globally Important Agricultural Heritage System
RF	FFRC No. 2 red carp
OJ	Oujiang color carp
F	fed
NF	non-fed
LSD	least significant difference
LEfSe	linear discriminant analysis effect size
LDA	linear discriminant analysis
PLS-DA	partial least squares discriminant analysis
PERMANOVA	permutational multivariate analysis of variance
PERMDISP	permutational analysis of multivariate dispersions
PCoA	principal coordinates analysis
PCA	principal component analysis
VIP	variable importance in projection
FDR	false discovery rate
DAMs	differentially abundant metabolites
OTU	operational taxonomic unit
ANOVA	analysis of variance
PIT	passive integrated transponder
SCFA	short-chain fatty acid
TCA	tricarboxylic acid (cycle)
CAMP	cationic antimicrobial peptide
PTS	phosphotransferase system
H&E	haematoxylin and eosin
MS-222	tricaine methanesulfonate
QC	quality control
SD	standard deviation
SRA	Sequence Read Archive

References

1. Kc, K.B.; Dias, G.M.; Veeramani, A.; Swanton, C.J.; Fraser, D.; Steinke, D.; Lee, E.; Wittman, H.; Farber, J.M.; Dunfield, K.; et al. When too much isn't enough: Does current food production meet global nutritional needs? *PLoS ONE* **2018**, *13*, e0205683. [CrossRef] [PubMed]
2. Tilman, D.; Cassman, K.G.; Matson, P.A.; Naylor, R.; Polasky, S. Agricultural sustainability and intensive production practices. *Nature* **2002**, *418*, 671–677. [CrossRef] [PubMed]
3. Wan, N.F.; Dainese, M.; Wang, Y.Q.; Loreau, M. Cascading social-ecological benefits of biodiversity for agriculture. *Curr. Biol.* **2024**, *34*, R587–R603, Erratum in *Curr. Biol.* **2026**, *36*, 3715. [CrossRef] [PubMed]
4. Wan, N.F.; Li, S.X.; Li, T.; Cavalieri, A.; Weiner, J.; Zheng, X.Q.; Ji, X.Y.; Zhang, J.Q.; Zhang, H.L.; Zhang, H.; et al. Ecological intensification of rice production through rice-fish co-culture. *J. Clean. Prod.* **2019**, *234*, 1002–1012. [CrossRef]
5. Wan, N.F.; Cavalieri, A.; Siemann, E.; Dainese, M.; Li, W.W.; Jiang, J.X. Spatial aggregation of herbivores and predators enhances tri-trophic cascades in paddy fields: Rice monoculture versus rice-fish co-culture. *J. Appl. Ecol.* **2022**, *59*, 2036–2045. [CrossRef]
6. Arunrat, N.; Sansupa, C.; Kongsurakan, P.; Sereenonchai, S.; Hatano, R. Soil microbial diversity and community composition in rice–fish co-culture and rice monoculture farming system. *Biology* **2022**, *11*, 1242. [CrossRef] [PubMed]
7. Sun, D.; Zheng, H.; Shi, Z.; Zhang, J.; Jia, Q.; Liu, X.; Zhao, M.; Chen, Y.; Chen, Q.; Luo, M. Rice-fish co-culture promotes soil carbon sequestration through alterations in soil microbial community structure. *Agronomy* **2025**, *15*, 1054. [CrossRef]
8. Rao, K.; Yang, L.; Sun, M.; Wu, C.; Guo, L.; Li, S.; Wu, D.; Xu, J. Effects of rice-fish co-culture models on sediment heavy metals, nutrient dynamics, and bacterial community structure. *Aquat. Ecol.* **2025**, *59*, 849–861. [CrossRef]
9. Nie, Z.; Xu, X.; Ji, Y.; Gao, P.; Zhou, S.; Sun, Y.; He, J.; Wang, L.; Shao, N.; Shi, Y. Rice-fish co-culture improves carp (*Cyprinus carpio*) quality by modulating the gut microbiota and metabolites. *Aquaculture* **2025**, *607*, 742659. [CrossRef]

10. He, Y.; Fu, B.; Fang, C.; Zhang, N.; Zheng, M.; Yang, Y.; Zhang, S.; Chen, S.; Yang, H. Decoding the gut-microbiota-muscle nexus: Multi-omics integration reveals mTOR driven flesh modulation in rice-fish co-cultured common carp (*Cyprinus carpio*). *Aquaculture* **2025**, *612*, 743090. [CrossRef]
11. Xie, J.; Hu, L.; Tang, J.; Wu, X.; Li, N.; Yuan, Y.; Yang, H.; Zhang, J.; Luo, S.; Chen, X. Ecological mechanisms underlying the sustainability of the agricultural heritage rice–fish coculture system. *Proc. Nati. Acad. Sci. USA* **2011**, *108*, E1381–E1387. [CrossRef] [PubMed]
12. Diao, W.; Yuan, J.; Jia, R.; Hou, Y.; Zhang, L.; Li, B.; Zhu, J. Integrated rice-fish culture alters the bacterioplankton community and its assembly processes. *Fishes* **2024**, *9*, 254. [CrossRef]
13. Shi, X.; Zhu, W.; Guo, J.; Lin, K.; Fu, J.; Wang, L.; Dong, Y.; Luo, M.; Dong, Z. Genome-wide association study reveals candidate genes critical for skin pigmentation in common carp (*Cyprinus carpio*) strains including *koi*. *Aquaculture* **2024**, *590*, 741075. [CrossRef]
14. Yang, N.; Tian, C.; Lv, Y.; Hou, J.; Yang, Z.; Xiao, X.; Zhang, Y. Novel primers for 16S rRNA gene-based archaeal and bacterial community analysis in oceanic trench sediments. *Appl. Microbiol. Biotechnol.* **2022**, *106*, 2795–2809. [CrossRef] [PubMed]
15. Edgar, R.C. Search and clustering orders of magnitude faster than BLAST. *Bioinformatics* **2010**, *26*, 2460. [CrossRef]
16. Prodan, A.; Tremaroli, V.; Brolin, H.; Zwinderman, A.H.; Nieuwdorp, M.; Levin, E. Comparing bioinformatic pipelines for microbial 16S rRNA amplicon sequencing. *PLoS ONE* **2020**, *15*, e0227434. [CrossRef] [PubMed]
17. Chen, S.; Zhou, Y.; Chen, Y.; Gu, J. fastp: An ultra-fast all-in-one FASTQ preprocessor. *Bioinformatics* **2018**, *34*, i884–i890. [CrossRef] [PubMed]
18. Li, D.; Luo, R.; Liu, C.M.; Leung, C.M.; Ting, H.F.; Sadakane, K.; Yamashita, H.; Lam, T.W. MEGAHIT v1.0: A fast and scalable metagenome assembler driven by advanced methodologies and community practices. *Methods* **2016**, *102*, 3–11. [CrossRef] [PubMed]
19. Hyatt, D.; Chen, G.L.; Locascio, P.F.; Land, M.L.; Larimer, F.W.; Hauser, L.J. Prodigal: Prokaryotic gene recognition and translation initiation site identification. *BMC Bioinform.* **2010**, *11*, 119. [CrossRef] [PubMed]
20. Steinegger, M.; Söding, J. Clustering huge protein sequence sets in linear time. *Nat. Commun.* **2018**, *9*, 2542. [CrossRef] [PubMed]
21. Buchfink, B.; Xie, C.; Huson, D.H. Fast and sensitive protein alignment using DIAMOND. *Nat. Methods* **2015**, *12*, 59–60. [CrossRef] [PubMed]
22. Chambers, M.C.; Maclean, B.; Burke, R.; Amodei, D.; Ruderman, D.L.; Neumann, S.; Gatto, L.; Fischer, B.; Pratt, B.; Egertson, J.; et al. A cross-platform toolkit for mass spectrometry and proteomics. *Nat. Biotechnol.* **2012**, *30*, 918–920. [CrossRef] [PubMed]
23. Wang, E.; Zhou, Y.; Liang, Y.; Ling, F.; Xue, X.; He, X.; Zhai, X.; Xue, Y.; Zhou, C.; Tang, G.; et al. Rice flowering improves the muscle nutrient, intestinal microbiota diversity, and liver metabolism profiles of tilapia (*Oreochromis niloticus*) in rice-fish symbiosis. *Microbiome* **2022**, *10*, 231. [CrossRef] [PubMed]
24. Kang, J.Y.; Chun, J.; Jahng, K.Y. Flavobacterium aciduliphilum sp. nov., isolated from freshwater, and emended description of the genus Flavobacterium. *Int. J. Syst. Evol. Microbiol.* **2013**, *63*, 1633–1638. [CrossRef] [PubMed]
25. Glaeser, S.P.; Kämpfer, P. The Family *Sphingomonadaceae*. In *The Prokaryotes*; Springer: Berlin/Heidelberg, Germany, 2014; pp. 641–707.
26. Satti, S.M.; Castro-Aguirre, E.; Shah, A.A.; Marsh, T.L.; Auras, R. Genome annotation of Poly (lactic acid) degrading *Pseudomonas aeruginosa*, *Sphingobacterium* sp. and *Geobacillus* sp. *Int. J. Mol. Sci.* **2021**, *22*, 7385. [CrossRef] [PubMed]
27. Cai, S.; Lv, W.; Zhu, H.; Zhang, D.; Fu, Z.; Zhang, H.; Xu, S. Effect of nitrogen application rate on soil fungi community structure in a rice-fish mutualistic system. *Sci. Rep.* **2019**, *9*, 16188. [CrossRef] [PubMed]
28. Hu, L.; Zhang, J.; Ren, W.; Guo, L.; Cheng, Y.; Li, J.; Li, K.; Zhu, Z.; Zhang, J.; Luo, S.; et al. Can the co-cultivation of rice and fish help sustain rice production? *Sci. Rep.* **2016**, *6*, 28728. [CrossRef] [PubMed]
29. Ren, W.; Hu, L.; Guo, L.; Zhang, J.; Tang, L.; Zhang, E.; Zhang, J.; Luo, S.; Tang, J.; Chen, X. Preservation of the genetic diversity of a local common carp in the agricultural heritage rice-fish system. *Proc. Natl. Acad. Sci. USA* **2018**, *115*, E546–E554. [CrossRef] [PubMed]
30. Luo, W.; Zhang, N.; Li, Z.; Xu, Z.; Wang, D.; Liao, G.; Pang, G.; Xu, G.; Wang, Y.; Huang, X.; et al. Increasement of Cd adsorption capacity of rice stubble from being alive until death in a modified rice-fish system. *Ecotoxicol. Environ. Saf.* **2021**, *208*, 111441. [CrossRef] [PubMed]
31. Tao, L.; Chai, J.; Liu, H.; Huang, W.; Zou, Y.; Wu, M.; Peng, B.; Wang, Q.; Tang, K. Characterization and dynamics of the gut microbiota in rice fishes at different developmental stages in rice-fish coculture systems. *Microorganisms* **2022**, *10*, 2373. [CrossRef] [PubMed]
32. Fu, M.; Kuang, R.; Wang, W.; Yu, Y.; Ai, T.; Liu, X.; Su, J.; Yuan, G. Hepcidin protects yellow catfish (*Pelteobagrus fulvidraco*) against aeromonas veronii-induced ascites disease by regulating iron metabolism. *Antibiotics* **2021**, *10*, 848. [CrossRef] [PubMed]
33. Zhang, X.H.; He, X.; Austin, B. *Vibrio harveyi*: A serious pathogen of fish and invertebrates in mariculture. *Mar. Life. Sci. Technol.* **2020**, *2*, 231–245. [CrossRef] [PubMed]

34. Nale, J.Y.; Ahmed, B.; Haigh, R.; Shan, J.; Phothaworn, P.; Thiennimitr, P.; Garcia, A.; AbuOun, M.; Anjum, M.F.; Korbsrisate, S.; et al. Activity of a Bacteriophage Cocktail to control *Salmonella Growth* Ex Vivo in avian, Porcine, and human epithelial cell cultures. *Phage* **2023**, *4*, 11–25. [CrossRef] [PubMed]
35. Zhao, Z.; Chu, C.; Zhou, D.; Wang, Q.; Wu, S.; Zheng, X.; Song, K.; Lv, W. Soil bacterial community composition in rice-fish integrated farming systems with different planting years. *Sci. Rep.* **2021**, *11*, 10855. [CrossRef] [PubMed]
36. Cheng, X.; Li, F.; Kumilamba, G.; Liao, J.; Cao, J.; Sun, J.; Liu, Q. Transcriptome analysis in hepatopancreases reveals the response of domesticated common carp to a high-temperature environment in the agricultural heritage rice-fish system. *Front. Physiol.* **2023**, *14*, 1294729. [CrossRef] [PubMed]

Disclaimer/Publisher's Note: The statements, opinions and data contained in all publications are solely those of the individual author(s) and contributor(s) and not of MDPI and/or the editor(s). MDPI and/or the editor(s) disclaim responsibility for any injury to people or property resulting from any ideas, methods, instructions or products referred to in the content.